All optical implementation scheme for Quantum Fourier Transform using polarization and orbital angular momentum of light

Akshay Menon P

A dissertation submitted for the partial fulfilment of BS-MS dual degree in Science

Indian Institute of Science Education and Research, Mohali

June 9, 2020

Certificate of Examination

This is to certify that the dissertation titled **"All optical implementation scheme for Quantum Fourier Transform using polarization and orbital angular momentum of light"** submitted by **Mr. Akshay Menon P** (Reg. No. MS15185) for the partial fulfilment of BS-MS dual degree programme of the Institute, has been examined by the thesis committee duly appointed by the Institute. The committee finds the work done by the candidate satisfactory and recommends that the report be accepted.

Dr. Kinjalk Lochan Dr. Sanjib Dey Dr. Sandeep K. Goyal

(Supervisor)

Date: June 9, 2020

Declaration

The work presented in this dissertation has been carried out by me under the guidance of Dr. Sandeep K. Goyal at the Indian Institute of Science Education and Research Mohali.

This work has not been submitted in part or in full for a degree, a diploma, or a fellowship to any other university or institute. Whenever contributions of others are involved, every effort is made to indicate this clearly, with due acknowledgement of collaborative research and discussions. This thesis is a bonafide record of original work done by me and all sources listed within have been detailed in the bibliography.

Akshay Menon P
Dated: June 9, 2020

In my capacity as the supervisor of the candidate's project work, I certify that the above statements by the candidate are true to the best of my knowledge.

Sandeep K. Goyal
Dated: June 9, 2020

Acknowledgements

I want to express my immense gratitude for my mentor Dr. Sandeep K. Goyal, for being a guiding lamp throughout the process of making this thesis a reality. He has been a great source of motivation and hope during harshly realistic times, and his simple insights into seemingly unsolvable problems opened up a whole new perspective, which was never thought of before. His continued support on academic as well as personal matters has helped me to remold myself as a good researcher, or a better individual.

I thank Dr. Ameen Yasir for detailed and insightful discussions on the generation and manipulation of structured light beams, which has helped me to deepen my knowledge about the same. Moreover, he has been a great friend and a meticulous critic of parts of this work.

I thank my parents and my sister for being a constant source of support and for understanding my perspectives which has helped greatly for completing my years in IISER Mohali. I would like to thank my best friend Anjana, for being with me through thick and thin, and for being a source of inspiration whenever I felt overwhelmed. I also thank my close friends, Chithra, Fidha and Swathi for helping me stay motivated throughout the writing process of this thesis. I thank everyone at IISER Mohali for making college a wonderful enriching experience.

Finally I would like to thank IISER Mohali for nurturing me to who I am today and DST-INSPIRE for providing financial support.

Akshay

List of Figures

Contents

Abstract

Internal modes of light can be used for efficient realization of any discrete arbitrary unitary matrix. For n_s spatial modes and n_i internal modes of light, we present a scheme for realizing $(n_s n_i) \times (n_s n_i)$ dimensional Quantum Fourier Transform (QFT) matrix. A generalized scheme for decomposing QFT matrix into physically realizable matrices corresponding to spatial and internal transformations is developed and then demonstrated for various choices of spatial and internal modes in realizing four-dimensional, eight-dimensional and twelve-dimensional QFT matrices. This decomposition reduces the number of beam splitters required for implementing QFT matrices, with an addition of internal transformations. Furthermore, implementation of the permutation matrices involved in realization of QFT are investigated.

Chapter 1

Introduction

Quantum algorithms claim an exponential speedup over their classical counterparts. This exponential speedup was demonstrated through various algorithms like Deutsch-Jozsa algorithm [Deutsch 92], and Shor's factoring algorithm [Shor 97]. The latter requires Quantum Fourier Transform (QFT) operations as a building block of the algorithm. QFT operations are also essential for Iterative Phase Estimation for finding eigenvalues of an arbitrary unitary matrix [Zhou 13]. Thus, implementing QFT experimentally is of great interest.

Implementing a discrete Fourier transform using quantum states is referred to as Quantum Fourier Transform. Many such implementations in various platforms like NMR quantum computer, Cavity-QED, superconducting qubits and Photonic chips were previously investigated [Weinstein 01, Scully 02, Mariantoni 11, Crespi 16]. In this work, we mainly focus on using linear optical setups for implementation of desired unitary transformations on a light beam.

In 1994, Reck *et al.* showed that linear optical elements like beam splitters and phase shifters can be used to approximate the action of an arbitrary finite-dimensional discrete unitary matrix [Reck 94]. This was accomplished by re-expressing N- dimensional unitary matrices as a sequence of two-dimensional beam splitter and phase shifter matrices. We will refer to this process of re-expressing a matrix as a product of two or more matrices as decomposition throughout this work. Their scheme required $\mathcal{O}(N^2)$ number of beam splitters to perform the desired N-dimensional unitary transformation on light. Later, in 2016, Clements *et al.* perfected this scheme to improve its scalability, but still required aligning $\mathcal{O}(N^2)$ number of beam splitters to achieve the desired unitary transformation [Clements 16]. Beam splitters tend to be lossy in realistic conditions. Moreover, aligning $\mathcal{O}(N^2)$ number of beam splitters as N increases is a practically difficult task. The obvious solution to overcome this problem is to reduce the number of beam splitters required for implementation.

In order to address this problem, Dhand *et al.* proposed a new algorithm which explored the use of various degrees of freedom (DOFs) of light to perform a desired

unitary transformation. Their scheme used internal modes of light like polarization, orbital angular momentum (OAM) and time bins to perform unitary transformations, along with the spatial modes of light used by Reck's and Clements' schemes. For an arbitrary $N = n_s n_p$-dimensional discrete unitary matrix, their scheme reduced the number of beam splitters by a factor of $n_p^2/2$, with a two-fold increase in the number of optical elements required for transformation of the internal modes [Dhand 15]. Here, n_s corresponds to the number of spatial modes and n_p corresponds to the number of internal modes of light.

In this work, we are interested in the implementation of QFT, which is an instance of a symmetric unitary matrix. In 1996, Torma *et al.* recognized that this symmetry can be exploited and introduced a new decomposition scheme which required considerably lesser number of beam splitters for realizing symmetric unitary transformations [Törmä 96].They managed to reduce the number of beam splitters required to $\mathcal{O}(Nlog_2N)$ for the specific case where N is a power of two. We adapt this decomposition method to include the internal modes of light, which is advantageous in further reducing the number of beam splitters required for implementation.

By using polarization and OAM of light alongside its spatial DOF to implement QFT operation, we require only six beam splitters for realization of an eight-dimensional QFT, as opposed to 12 beam splitters required by Torma's scheme. A major difficulty for actual implementation of the proposed scheme stems from the permutation matrices involved in the decomposition, which was not considered explicitly in the previous work [Törmä 96]. Next, we present a setup for the particular case of twelve-dimensional QFT, in which a new way of realizing a three-dimensional QFT on OAM modes is devised. The permutation matrix associated with twelve dimensions is hard to implement, suggesting that we still require a general decomposition for arbitrary N-dimensional permutations in terms of spatial and internal modes of light. We also take note of the modularity presented by Torma's scheme and investigate how it can be of use in realization of QFT matrices with internal modes of light.

The result that we present in this work will be helpful for an easy implementation of higher dimensional QFT, which may be helpful in data post-processing for emerging quantum machine learning schemes[Lloyd 13], quantum arithmetic[Ruiz-Perez 17], and solving hidden subgroup problems [Roetteler 98].

This thesis is organized into 4 chapters. Chapter 2 contains detailed discussions regarding the relevant background required, which includes unitary matrix implementation by Reck *et al.* and Clements *et al.* and Dhand *et al.*, along with the adapted version of Torma *et al.* implementation of QFT so as to include internal DOFs of light. This chapter also contains discussions on methods used to implement unitary

transformations on polarization and OAM DOFs of light. Possible applications of our adaptation and various experimental implementations of selected QFT matrices are presented in Chapter 3. This chapter also includes a cost analysis with respect to the number of optical elements required for implementation of QFT. Further discussions including possible use cases of the algorithm and challenges ahead constitute Chapter 4.

Chapter 2

Background

In classical optics, light beams are characterized by its electric field components. Every optical element acts on the input electric field component of light to perform a linear transformation on the beam. This means that the action of these optical elements can be quantified by means of unitary matrices. Unitarity of the matrix implies that the intensity of the input light beam is unchanged by the action of the optical element.

Similarly, in Quantum Optics, optical elements transform the creation or annihilation operators related to the electric field components of the input light beam, to that of the output beam. Here, unitarity of the transformation matrix is related to preservation of probability amplitudes of the input quantum states. In this chapter, we will discuss about different experimental schemes used for implementing unitary transformations in various DOFs of light.

2.1 Unitary matrices

Unitary matrices of finite dimension N are complex square matrices which satisfies the relation

$$UU^{\dagger} = U^{\dagger}U = \mathbb{1}. \tag{2.1}$$

Imposing an additional constraint that $det|U| = 1$ results in the special unitary matrix. A group of such N-dimensional unitary matrices with the group operation of multiplication constitutes the Special Unitary group (denoted as $\mathbb{SU}(N)$). It is well known that $\mathbb{SU}(2)$ is homomorphic to $\mathbb{SO}(3)$, which is the special orthogonal group corresponding to three-dimensional rotations. The general form of a matrix belonging to $\mathbb{SU}(2)$ can be written as

$$U = \begin{bmatrix} \eta & \chi \\ -\chi^{*} & \eta^{*} \end{bmatrix}, \tag{2.2}$$

with $\eta = a + ib$, $\chi = c + id$, and $a^2 + b^2 + c^2 + d^2 = 1$. This means that it requires three independent parameters to define an element of the $\mathbb{SU}(2)$ group. A commonly used parameterization for $\mathbb{SU}(2)$ is in terms of Euler angles. For angles α, β, and γ,

$$U(\alpha, \beta, \gamma) = e^{-\frac{i}{2}\alpha\sigma_2} e^{\frac{i}{2}\beta\sigma_3} e^{-\frac{i}{2}\gamma\sigma_2} \tag{2.3}$$

where σ_2 and σ_3 are Pauli matrices. We will now see how $\mathbb{SU}(2)$ operations are physically implemented on light beams.

2.2 $\mathbb{SU}(2)$ operations on different DOFs of light

A single photon can be associated with various DOFs. The path in which the photon is localized is referred to as the spatial DOF. The input and output ports of a beam splitter can be considered as the spatial DOF accessible by a photon.

A single photon can be associated with different mutually orthogonal polarization states. This corresponds to the polarization DOF of the photon. Usually, the horizontal and vertical polarization are chosen as the basis for representing polarization DOF. Similarly, a single photon can carry a superposition of l OAM states, where l is an unbounded integer. This is referred to as the OAM DOF of photon.

2.2.1 Spatial DOFs

Specific $\mathbb{SU}(2)$ operations can be performed on the spatial DOFs of photons using a Mach-Zehnder Interferometer (MZI) combined with a phase shifter. A MZI consists of two each of beam splitters, phase shifters and mirrors. This is used as the building block of some of the schemes that use spatial DOF of light to implement unitary transformations. A beam splitter is a four-port device, with two input ports and two output ports. These ports corresponds to the spatial modes of the incoming photons. A beam splitter with 50% transmittance and 50% reflectance can be represented as

$$B = \frac{1}{\sqrt{2}} \begin{bmatrix} 1 & i \\ i & 1 \end{bmatrix}. \tag{2.4}$$

As the name suggests, a phase shifter acts on the beam to impart a phase difference, say ϕ_k, between the input and output beams. The matrix corresponding to a phase shifter is thus

$$P = \begin{bmatrix} e^{i\phi_1} & 0 \\ 0 & e^{i\phi_2} \end{bmatrix}. \tag{2.5}$$

In the case of a MZI, we only require one phase shifter in one of the arms (as this imparts the relative phase difference between the two arms of the interferometer), as

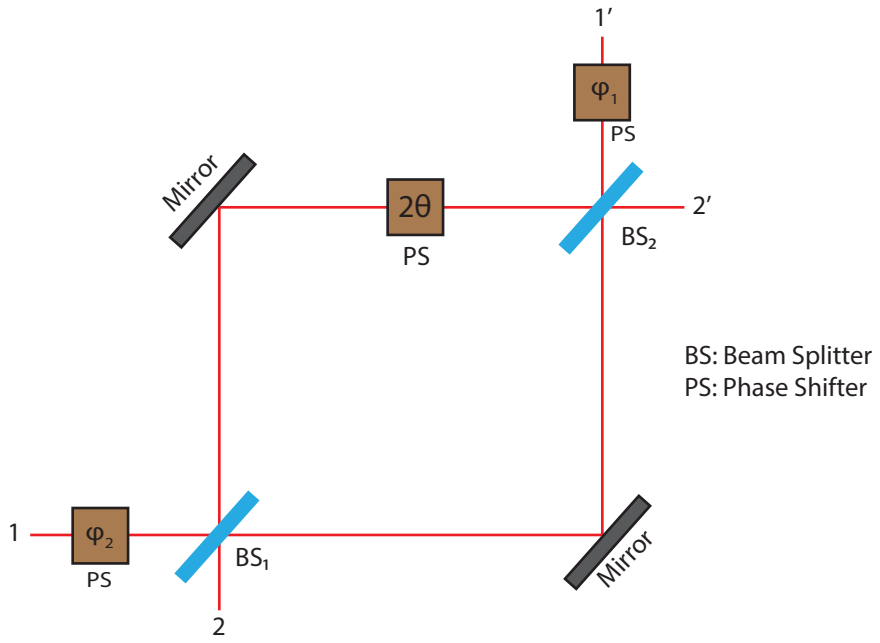

Figure 2.1: $\mathbb{SU}(2)$ *operation on spatial DOFs*: A MZI with two different phase shifters at the first input and output ports imparts a $\mathbb{SU}(2)$ transformation on the spatial DOFs. Adding a phase element to both of the output ports will result in a $\mathbb{U}(2)$ transformation.

shown in Fig 2.1. The matrix representation of the interferometer thus becomes,

$$\begin{aligned} T &= B^{\dagger}PB \\ &= \frac{1}{2}\begin{bmatrix} 1 & -i \\ -i & 1 \end{bmatrix}\begin{bmatrix} e^{i2\theta} & 0 \\ 0 & 1 \end{bmatrix}\begin{bmatrix} 1 & i \\ i & 1 \end{bmatrix} \\ &= \frac{1}{2}\begin{bmatrix} e^{i2\theta}+1 & ie^{i2\theta}-i \\ -ie^{i2\theta}+i & e^{i2\theta}+1 \end{bmatrix} \\ &= \frac{e^{i\theta}}{2}\begin{bmatrix} e^{i\theta}+e^{-i\theta} & i(e^{i\theta}-e^{-i\theta}) \\ -i(e^{i\theta}-e^{-i\theta}) & e^{i\theta}+e^{-i\theta} \end{bmatrix} \\ &= e^{i\theta}\begin{bmatrix} \cos\theta & \sin\theta \\ -\sin\theta & \cos\theta \end{bmatrix} \end{aligned} \tag{2.6}$$

Here, $e^{i\theta}$ is a global phase which changes the phase of every state equally, and thus can be omitted. Now, imparting a phase shift in one of the spatial modes,

$$T' = \begin{bmatrix} e^{i\phi} & 0 \\ 0 & 1 \end{bmatrix}\begin{bmatrix} \cos\theta & \sin\theta \\ -\sin\theta & \cos\theta \end{bmatrix} = \begin{bmatrix} e^{i\phi}\cos\theta & e^{i\phi}\sin\theta \\ -\sin\theta & \cos\theta \end{bmatrix} \tag{2.7}$$

It is easy to check that T' satisfies the relation in Eq.2.2, thus confirming that MZI combined with a phase shifter performs a $\mathbb{SU}(2)$ operation on the input beams. This

setup is used as a substitute for variable reflectivity beam splitters, as it is easier to tune θ and ϕ to the desired reflectivity and transmittance values of the required beam splitter.

Schemes using spatial DOF to implement a unitary transformation uses an array of MZIs paired with phase shifters to act as the desired unitary transformation. In Section 2.3, we see such algorithms that decompose a matrix into smaller $\mathbb{SU}(2)$ operations corresponding to MZI-Phase shifter pairs.

However, this setup is characterized by only two parameters, and hence does not impart any arbitrary $\mathbb{SU}(2)$ operation using the spatial DOF. Adding a phase shifter at one of the input ports of the MZI-phase shifter pair results in

$$T\text{"} = \begin{bmatrix} e^{i\phi_1}\cos\theta & e^{i\phi_1}\sin\theta \\ -\sin\theta & \cos\theta \end{bmatrix} \begin{bmatrix} e^{i\phi_2} & 0 \\ 0 & 1 \end{bmatrix} = \begin{bmatrix} e^{i(\phi_1+\phi_2)}\cos\theta & e^{i\phi_1}\sin\theta \\ -e^{i\phi_2}\sin\theta & \cos\theta \end{bmatrix} \tag{2.8}$$

T" is characterized by three independent parameters, and hence can perform any arbitrary $\mathbb{SU}(2)$ operation on the input light beam. An additional phase shifter can be added in the output spatial mode to impart any $\mathbb{U}(2)$ operation on the beam, as $\mathbb{SU}(2)$ and $\mathbb{U}(2)$ differs only in the global phase factor. Now, we see how $\mathbb{SU}(2)$ operations can be implemented using internal DOFs of light.

2.2.2 Internal DOFs

In 1989, Simon and Mukunda noted that a sequence of co-axially mounted Quarter-Wave Plates (QWPs) and Half-Wave Plates (HWPs) can be used to impart any desirable $\mathbb{SU}(2)$ transformation on the polarization DOF [Simon 89]. Waveplates are birefringent plates with a mutually orthogonal slow and fast axes. Waveplates delay the phase of the electric field component corresponding to fast axis by a certain amount, say ζ. Let the fast axis of the wavelpate be in y direction, slow axis be in x direction, and let the wave propagate through z direction. A general expression of a waveplate thus becomes,

$$W_0(\zeta) = e^{-i\zeta/2} \begin{bmatrix} e^{i\zeta/2} & 0 \\ 0 & e^{-i\zeta/2} \end{bmatrix} = e^{-i\zeta/2} e^{i\frac{\zeta}{2}\sigma_3}. \tag{2.9}$$

Suppressing the global phase factor $e^{-i\zeta/2}$, we see that $W_0(\zeta) \in \mathbb{SU}(2)$. The subscript denotes the angle between the slow axis and a unit vector along x direction. Any arbitrary rotation of the waveplate can be quantified by multiplication of the rotation matrix

$$R(\theta) = \begin{bmatrix} \cos\theta & -\sin\theta \\ \sin\theta & \cos\theta \end{bmatrix} = e^{-i\theta\sigma_2}, \tag{2.10}$$

so that

$$W_\theta(\zeta) = R(\theta)W_0(\zeta)R^{-1}(\theta) \tag{2.11}$$

Note that $R^{-1}(\theta) = R(-\theta)$. For any waveplate, rotation through an angle of π does not change the operation of the waveplate. However, rotation through an angle of $\pi/2$ interchanges the fast and slow axes, resulting in an inverse operation of the waveplate. Recall from Eq. 2.3 that any $\mathbb{SU}(2)$ matrix can be parameterized using Euler angles. In comparison with Eq. 2.9 and Eq. 2.10, we see that

$$\begin{aligned} U(\alpha,\beta,\gamma) &= R(\alpha/2)W_0(\beta/2)R(\gamma/2) \\ &= R(\alpha/2)W_0(\beta/2)R^{-1}(\alpha/2)R(\alpha/2)R(\gamma/2) \\ &= W_{\alpha/2}(\beta)R((\alpha+\gamma)/2) \end{aligned} \tag{2.12}$$

For a HWP, $\zeta = \pi$ and for a QWP, $\zeta = \pi/2$. Their corresponding matrices at $\theta = 0$ are

$$H_0 = \begin{bmatrix} i & 0 \\ 0 & -i \end{bmatrix} = i\sigma_3, \tag{2.13}$$

$$Q_0 = \begin{bmatrix} e^{i\pi/4} & 0 \\ 0 & e^{-i\pi/4} \end{bmatrix}. \tag{2.14}$$

As σ_2 and σ_3 are anti-commutative, it is straightforward to check that $H_0R(\theta) = R^{-1}(\theta)H_0$. Also, two-dimensional rotations commute with each other about the origin. Using these identities,

$$\begin{aligned} H_{\theta_0}H_{\theta_0\pm\pi/2-\theta/4} &= R(\theta_0)H_0R^{-1}(\theta_0)R(\theta_0\pm\pi/2)R^{-1}(\theta/4)H_0R(\theta/4)R^{-1}(\theta_0\pm\pi/2) \\ &= R(\theta_0)H_0R^{-1}(\theta_0)R(\theta_0\pm\pi/2)H_0R(\theta/2)R^{-1}(\theta_0\pm\pi/2) \\ &= R(\theta_0)H_0R^{-1}(\theta_0)R(\theta_0\pm\pi/2)H_0R^{-1}(\theta_0\pm\pi/2)R(\theta/2) \\ &= H_{\theta_0}H_{\theta_0\pm\pi/2}R(\theta/2) \qquad [\text{since } \mathrm{H}_{\theta_0}^{-1} = \mathrm{H}_{\theta_0\pm\pi/2}] \\ &= R(\theta/2). \end{aligned} \tag{2.15}$$

Similarly, it can be established that

$$H_{\theta_0\pm\pi/2+\theta/4}H_{\theta_0} = R(\theta/2). \tag{2.16}$$

Thus, we see that any arbitrary rotation of polarization can be achieved using a combination of two HWPs. This can be further simplified. Now, consider the expression

$$\begin{aligned} Q_{\pi/4}R(\beta/2)Q_{\pi/4}^{-1} &= R(\pi/4)Q_0R(-\pi/4)R(\beta/2)R(\pi/4)Q_0^{-1}R(-\pi/4) \\ &= R(\pi/4)Q_0R(-\pi/4)R(\pi/4)R(\beta/2)Q_0^{-1}R(-\pi/4) \\ &= R(\pi/4)Q_0R(\beta/2)Q_0^{-1}R(-\pi/4) \\ &= R(\pi/4)e^{i\frac{\pi}{4}\sigma_3}e^{-i\frac{\beta}{2}\sigma_2}e^{i\frac{\pi}{4}\sigma_3}R(-\pi/4). \end{aligned} \tag{2.17}$$

Taking note of the fact that $\sigma_2\sigma_3 = i\sigma_1 = -\sigma_3\sigma_2$,

$$Q_{\pi/4}R(\beta/2)Q_{\pi/4}^{-1} = R(\pi/4)e^{-i\frac{\beta}{2}\sigma_1}R(-\pi/4). \tag{2.18}$$

Rotating $-\sigma_1$ through $\pi/4$ results in σ_3, which implies

$$Q_{\pi/4}R(\beta/2)Q_{\pi/4}^{-1} = e^{i\frac{\beta}{2}\sigma_3}. \tag{2.19}$$

Multiplying both sides of Eq. 2.19 with $e^{-i\frac{\alpha}{2}\sigma_2}$ from left and $e^{i\frac{\alpha}{2}\sigma_2}$ from right,

$$Q_{\alpha/2+\pi/4}R(\beta/2)Q_{\alpha/2+\pi/4}^{-1} = e^{-i\frac{\alpha}{2}\sigma_2}e^{i\frac{\beta}{2}\sigma_3}e^{i\frac{\alpha}{2}\sigma_2}. \tag{2.20}$$

Combining Eq. 2.15, Eq. 2.16 and Eq. 2.20, Eq. 2.12 can be re-expressed as

$$U(\alpha,\beta,\gamma) = Q_{\alpha/2+\pi/4}H_{\theta_0\pm\pi/2+\beta/4}H_{\theta_0}Q_{\alpha/2+\pi/4}^{-1}H_{\xi_0}H_{\xi_0\pm\pi/2-(\alpha+\gamma)/4}. \tag{2.21}$$

The value of θ_0 and ξ_0 in this expression can be carefully chosen so that the number of parameters is reduced to three, as required for describing an arbitrary $\mathbb{SU}(2)$ matrix. This choice can be made by noting that aligning the principal directions of H_{θ_0} and H_{ξ_0} to that of $Q_{\alpha/2+\pi/4}^{-1} = Q_{\alpha/2-\pi/4}$ lets these matrices commute with each other. This means that $\theta_0 = \alpha/2 \pm \pi/4$ and $\xi_0 = \alpha/2 \mp \pi/4$, which leads to

$$\begin{aligned} U(\alpha,\beta,\gamma) &= Q_{\alpha/2+\pi/4}H_{\alpha/2\mp\pi/4+\beta/4}Q_{\alpha/2-\pi/4}H_{\alpha/2\pm\pi/4}H_{\alpha/2\mp\pi/4}H_{\alpha/2\pm\pi/4-(\alpha+\gamma)/4} \\ &= Q_{\alpha/2+\pi/4}H_{\alpha/2\mp\pi/4+\beta/4}Q_{\alpha/2-\pi/4}H_{\alpha/2\pm\pi/4}H_{\alpha/2\pm\pi/4}^{-1}H_{\alpha/2\pm\pi/4-(\alpha+\gamma)/4} \\ &= Q_{\alpha/2+\pi/4}H_{\alpha/2\mp\pi/4+\beta/4}Q_{\alpha/2-\pi/4}H_{(\alpha-\gamma)/4\pm\pi/4}. \end{aligned} \tag{2.22}$$

Using the same identities as in Eq. 2.15, a general combination of waveplates H_ξ,

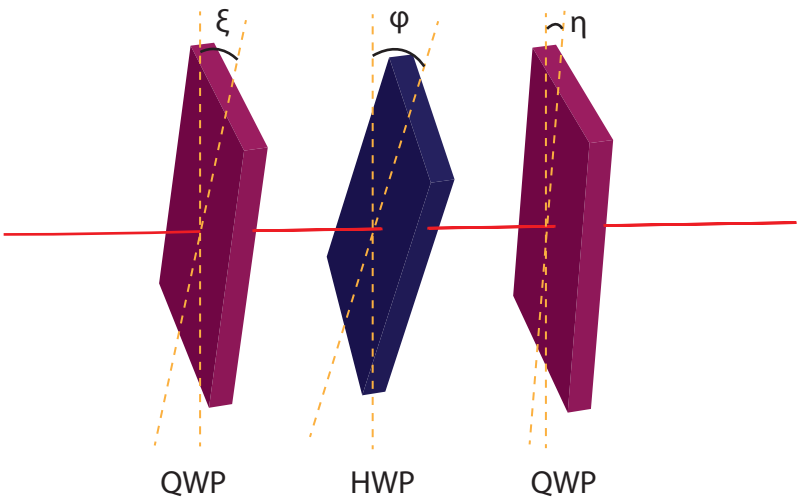

Figure 2.2: *Simon-Mukunda polarization gadget*: Two QWPs and a HWP oriented at respective angles suffices to impart any arbitrary $\mathbb{SU}(2)$ operation on the polarization modes of light. Note that the waveplates are co-axially mounted.

Q_ϕ, and H_η can be expressed as

$$\begin{aligned} H_\xi Q_\phi H_\eta &= H_\xi R(\phi) Q_0 R(-\phi) R(\eta) H_0 R(-\eta) \\ &= H_\xi R(\phi) Q_0 R(-\phi) H_0 R(-2\eta) \\ &= H_\xi R(\phi) Q_0 H_0 R(-(2\eta - \phi)) \\ &= H_\xi R(\phi) R(\pi) Q_{\pi/2} R(-(2\eta - \phi)). \end{aligned} \tag{2.23}$$

Introducing $\mathbb{1} = R(-(2\eta - \phi))R((2\eta - \phi))$ to this equation,

$$\begin{aligned} H_\xi Q_\phi H_\eta &= H_\xi R(\phi + \pi) R(-(2\eta - \phi)) R((2\eta - \phi)) Q_{\pi/2} R(-(2\eta - \phi)) \\ &= H_\xi R(2(\phi - \eta + \pi/2)) Q_{2\eta - \phi + \pi/2} \\ &= H_\xi R(2(\phi - \eta + \pi/2)) Q_{2\eta - \phi + \pi/2} \\ &= R(-(\phi - \eta + \pi/2)) H_\xi R(\phi - \eta + \pi/2) Q_{2\eta - \phi + \pi/2} \\ &= H_{\xi - \phi + \eta - \pi/2} Q_{2\eta - \phi + \pi/2}. \end{aligned} \tag{2.24}$$

Using Eq. 2.24, we can further simplify Eq. 2.22 as

$$U(\alpha, \beta, \gamma) = Q_{\alpha/2 + \pi/4} H_{(\alpha + \beta - \gamma)/4 - \pi/4} Q_{\pi/4 - \alpha/4}. \tag{2.25}$$

This means that any arbitrary $\mathbb{SU}(2)$ operation on polarization can be realized by co-axially mounting two QWPs and a HWP. The values of α, β and γ can be found for the desired unitary matrix through Euler decomposition and then the waveplates can be arranged accordingly. Fig. 2.2 illustrates the experimental setup used. Simon and Mukunda have also proved that any combination of two QWPs and a HWP can

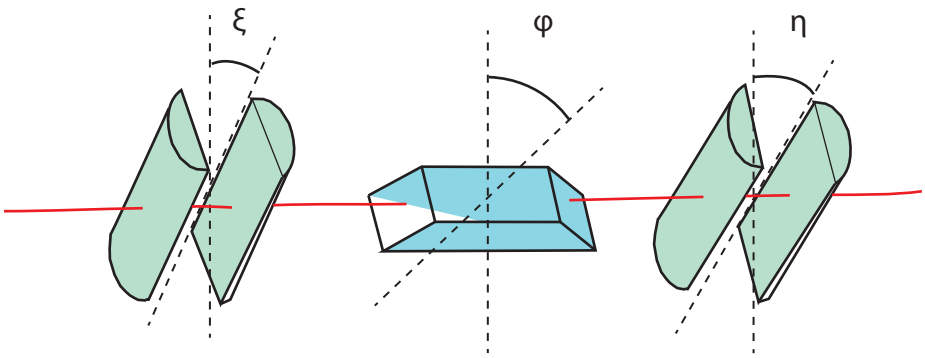

Figure 2.3: $\mathbb{SU}(2)$ *operation on OAM*: Device similar to Simon-Mukunda polarization gadget for performing $\mathbb{SU}(2)$ operation on OAM modes with N=1

be used for experimental realization of $\mathbb{SU}(2)$ operations [Simon 90].

A much more versatile internal DOF is the OAM carried by light beams. In 1992, Allen *et al.* showed that a paraxial linearly polarized Laguerre-Gaussian (LG) beam can have a $\exp(il\theta)$ phase dependence, with $l\hbar$ being the value of OAM carried per photon [Allen 92]. Here, l is an integer which is unbounded, which implies that a single photon can be associated to an infinite dimensional Hilbert space. LG beams have a helical wavefront and are analogous to circularly polarized light. Similarly, another class of beams known as Hermite-Gaussian (HG) beams are analogous to linear polarization.

Following Allen's work, Beijersbergen *et al.* noted that an arrangement of cylindrical lenses (known as Astigmatic mode converters) can impart a Gouy phase shift (phase shift suffered by the beam passing through the waist of the Gaussian beam as compared with a plane wave) to the input beam, thus enabling inter-conversion of a rotated HG beam to LG beam or vice-versa [Beijersbergen 93]. This setup is referred to as a $\pi/2$-mode converter, as it introduces a phase shift of $\pi/2$ between successive terms in the expansion of either rotated HG beam or LG beam. It was duly noted that the matrix for of a $\pi/2$-mode converter is

$$C(\pi/2) = \begin{bmatrix} 1 & & & & & & \\ & -i & & & & & \\ & & -1 & & & & \\ & & & i & & & \\ & & & & 1 & & \\ & & & & & -i & \\ & & & & & & \ddots \end{bmatrix}, \tag{2.26}$$

by Allen *et al.* [Allen 99]. The matrix is infinite dimensional owing to unbounded values of l. In the case of two OAM modes, we see that this action is analogous to

that of a QWP on a linearly polarized light. Another important optical element that transforms OAM is the Dove prism. A Dove prism adds a l dependent phase to the input beam, depending on the orientation angle of the prism ($\exp(i\alpha l)$, where α is the orientation angle). An input beam impinging on the Dove prism undergoes two refractions and a total internal reflection before emerging at the output [Moreno 04]. This effectively rotates the beam based on the orientation angle of the prism.

Later, Gadway *et al.* noted that two $\pi/2$-mode converters and a Dove prism (Fig. 2.3) can be used analogously to the Simon-Mukunda polarization gadget to impart any $\mathbb{SU}(2)$ transformation on selected l values ($l = \pm 1$)[Gadway 08]. This constraint is inherent to the mode converter design, as discussed in [Beijersbergen 93]. We discuss the details of the origin of these values of orbital angular momentum with reference to Schwinger's representation in Section 2.7.

2.3 Implementation of unitary matrices using spatial modes

Conventionally, the experimental realization of a N-dimensional arbitrary discrete unitary matrix is achieved by expressing it as a product of smaller dimensional matrices corresponding to transformation matrices of optical elements. This process of re-expressing a matrix as a product of matrices is referred to as decomposition. An important milestone in devising experimental setups for unitary matrix realization was due to Reck *et al.* [Reck 94]. According to their scheme, the physical representation of a N-dimensional unitary matrix would have N input and output ports respectively. The algorithm which they devised for decomposing any arbitrary unitary matrix is as follows

1. Take as input the N-dimensional arbitrary unitary matrix U, which is to be decomposed.

2. Define

$$T_{p,q}(\theta,\phi) = \begin{bmatrix} 1 & & & & & & \\ & \ddots & & & & & \\ & & \cos\theta\, e^{i\phi} & \cdots & \sin\theta\, e^{i\phi} & & \\ & & \vdots & \ddots & \vdots & & \\ & & -\sin\theta & \cdots & \cos\theta & & \\ & & & & & \ddots & \\ & & & & & & 1 \end{bmatrix}, \tag{2.27}$$

   which matches the dimensions of U. Note that the entries that are embedded in the p^{th} and q^{th} rows and columns of $T_{p,q}(\theta,\phi)$ corresponds to a MZI matrix

(as in Eq. 2.6) multiplied by a phase shifter matrix imparting a phase shift of ϕ to the first output mode of MZI respectively (the inverse of this matrix is denoted as $T_{p,q}^{-1}(\theta, \phi)$). This matrix only affects a two-dimensional subspace of the N-dimensional matrix U.

3. Multiply U with $T_{N,N-1}(\theta, \phi)$ from the right by choosing appropriate values for θ and ϕ, such that $(N, N-1)^{th}$ element of U is nulled.

4. Repeat this procedure so that

$$UT_{N,N-1}T_{N,N-2}\dots T_{2,1} = D, \tag{2.28}$$

where D is a diagonal unitary matrix. We have omitted (θ, ϕ) to simplify the notation. This let's us write the matrix U as

$$U = DT_{2,1}^{-1}\dots T_{N,N-2}^{-1}T_{N,N-1}^{-1}, \tag{2.29}$$

which completes the decomposition.

From a physical point of view, the matrix $T_{N,N-1}(\theta, \phi)$ represents a variable reflectivity beam splitter acting on the input ports N and $N-1$. It is easy to see that $\binom{N}{2}$ operations are required to null the lower triangular part of matrix U. So, this decomposition method results in an experimental setup that utilizes N spatial modes, on which $N(N-1)/2$ beam splitter devices are arranged in a triangular array, along with appropriate phase shifts dictated by D where necessary (Fig. 2.4.b).

This method of implementing unitary matrix suffers when the dimensionality of the matrix U increases, as aligning $\mathcal{O}(N^2)$ beams splitters perfectly becomes a tedious task and the setup suffers from loss in fidelity of the output states. One of the main reason for this loss is that a beam encounters different number of optical elements in each spatial mode due to the triangular pattern in which the elements are ordered. This creates an unbalanced loss along different arms of the setup. In order to tackle the problem of unbalanced loss, Clements et. al. put forth a new decomposition algorithm. Their algorithm is similar to Reck's except for the third step where diagonalization of U begins. Instead of diagonalizing U by multiplying appropriate $T_{p,q}(\theta, \phi)$ only from the right, Clements *et al.* also multiplies U with $T_{p,q}^{-1}(\theta, \phi)$ from the left, under the constraint that only nearest neighbour p and q are chosen. This step changes the order in which the elements of the lower triangular part of U is nulled, which translates into a more compact rectangular array of beam splitter devices over the triangular array proposed by Reck et. al.(Fig.2.4.c). The algorithm can be summed up as

1. Take as input the N-dimensional unitary matrix U.

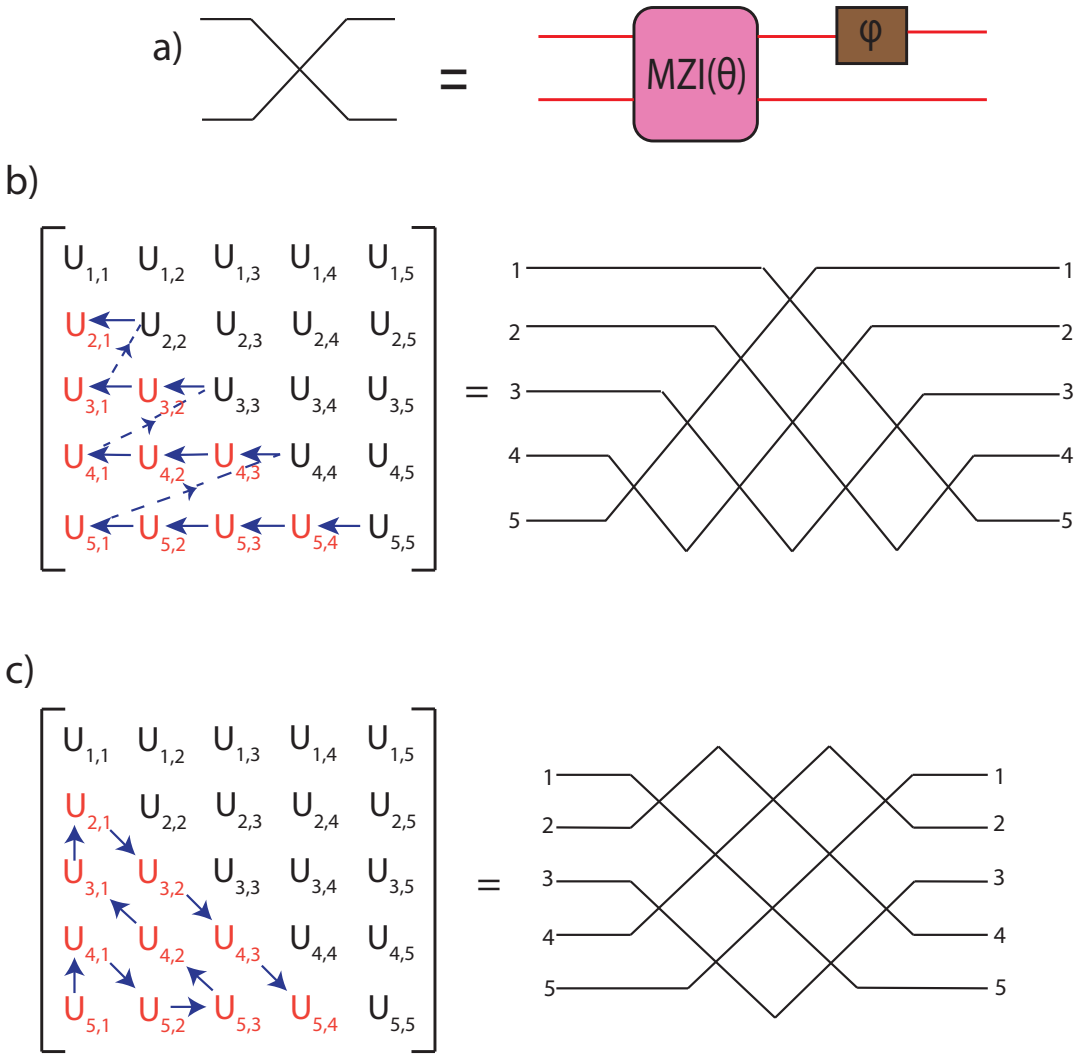

Figure 2.4: *Optical architectures*: Architectures arising due to Reck's and Clements' decomposition is compared in this figure. a) Simplification used for representing the variable reflectivity beam splitter device. Here, straight lines corresponds to the optical modes and X shaped structure corresponds to the beam splitter device (which is a composition of a MZI and a phase shifter). V shaped structure corresponds to a mirror reflection. b) Reck's scheme. c) Clement's scheme. Red elements are nulled in both the schemes and blue arrows show the order in which the elements are nulled. Adjacent to it is the experimental setup resulting from arranging the beam splitter devices as in the decomposition sequence. A specific case of $N = 5$ is used here to illustrate both algorithms. Note that Reck's scheme generates a triangular array of beam splitter devices while Clements' scheme generates a rectangular array of beam splitter devices.

2. Define an iterable, say k, which ranges in $[1, N-1]$.

3. If k is odd, then

   (a) Define an iterable, say j, which ranges in $[0, k-1]$.

   (b) Find a matrix $T_{k-j,k-j+1}(\theta, \phi)$, with appropriate values for θ and ϕ which nulls the element $(N-j, k-j)$

   (c) Multiply U from left with $T_{k-j,k-j+1}(\theta, \phi)$, so that

$$U = UT_{k-j,k-j+1}(\theta, \phi). \tag{2.30}$$

4. If k is even, then

   (a) Define an iterable, say j, which ranges in $[0, k]$.

   (b) Find a matrix $T^{-1}_{N+j-k-1,N+j-k}(\theta, \phi)$, with appropriate values for θ and ϕ which nulls the element $(N+j-k, j)$

   (c) Multiply U from right with $T^{-1}_{N+j-k-1,N+j-k}(\theta, \phi)$, so that

$$U = T^{-1}_{N+j-k-1,N+j-k}(\theta, \phi)U. \tag{2.31}$$

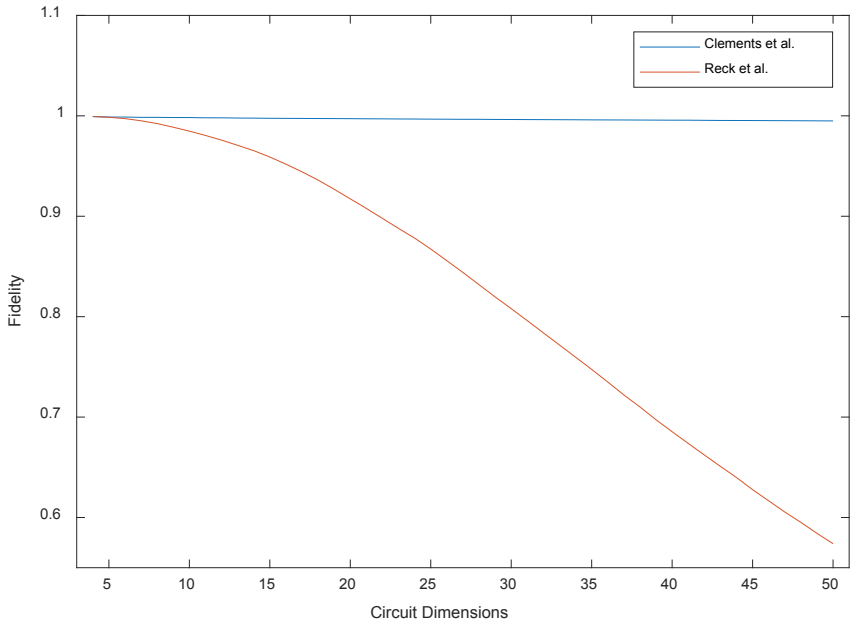

Figure 2.5: *Comparison of fidelities*: Output fidelities simulated for Reck's method and Clement's method, with a 2% loss in intensity at each beam splitter. As the dimensionality of the unitary matrix increases, beam splitters also increase. Balanced loss presented by Clement's method stabilizes over a fidelity of 1 without much loss, in contrast to a steep drop in fidelity for Reck's method.

This method claimed to have balanced loss due to its rectangular structure, as the beam now encounters similar number optical elements along different spatial modes, making it an optimal architecture for realization of unitary matrices [Clements 16]. The fidelity of the optical circuit can be calculated according to

$$F = \left| \frac{tr(U^{\dagger} U_{exp})}{\sqrt{N tr(U_{exp}^{\dagger} U_{exp})}} \right|^2 , \tag{2.32}$$

where U_{exp} corresponds to multiplication of all matrices in the decomposition. As a standard metric, higher values of F corresponds to lesser loss due to the circuit. We observe that the decline in fidelity is far less for Clement's scheme as compared to Reck's scheme (Fig. 2.5). Also, the rectangular array made the optical depth of the circuit much less as compared to Reck's scheme. However, the practical difficulty in aligning $\mathcal{O}(N^2)$ beam splitters still remained a problem.

2.4 OAM sorter

The ability to perform N-dimensional arbitrary unitary operation on OAM modes can be achieved through a setup known as OAM sorter [Leach 02]. The OAM sorter consists of a Mach-Zehnder interferometer setup with Dove prisms in both of its arms. As we have noted in Section 2.2.2, OAM carrying beams have a l-dependent phase given by $\exp(il\phi)$. The Dove prisms in the OAM sorter are rotated at a relative angle of $\alpha/2$, and is responsible for performing rotation on the incoming beam by an amount α, so that the the phase difference between the original beam and rotated beam is $l\alpha$. Specific combinations of l and α let's us choose the modes to be in phase with each other or out-of-phase with each other.

Fixing the value of $\alpha = \pi$, we see that rotated even OAM modes are in phase with their corresponding original beam in one arm of the MZI, while the odd modes in the same arm are out of phase with the original beam. This creates constructive interference of even OAM modes and destructive interference of odd OAM modes. The exact opposite happens in the other arm of the interferometer. Thus, we get even OAM modes through output port 1 and odd OAM modes through output port 2.

The same setup can be used again at the two output ports to perform further sorting of OAM values. In the next stage, α is set to $\pi/2$, so that even and odd OAM values exit through different ports of the OAM sorter. This can be carried out recursively until all N OAM modes are separated from the superposition.

After achieving spatial separation of OAM modes through cascaded use of OAM sorters, we can now use SLMs to generate an arbitrary superposition of states in different spatial modes. Hence, for realizing a N-dimensional unitary transformation

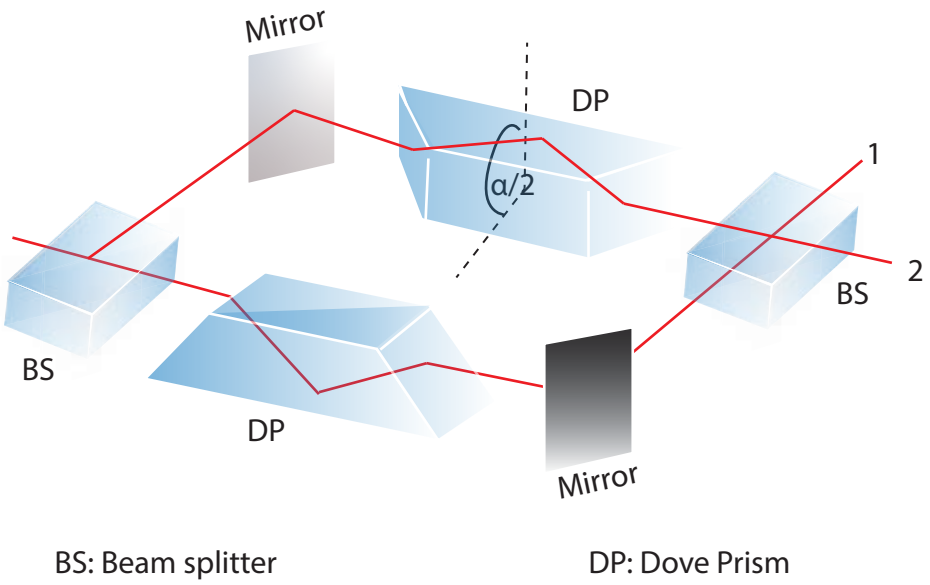

Figure 2.6: *OAM sorter*: The setup used for implementing an OAM sorter. A MZI with Dove prisms on its both arms are used to perform sorting. To sort even and odd OAM values, the value of the relative rotation angle between the Dove prisms, α, is set to π. Even values of OAM are sorted to port 1 and odd values of OAM are sorted to port 2.

on OAM modes, we require $(N-1)$ OAM sorters and N SLMs. This means that we need $2(N-1)$ number of beam splitters, Dove prisms and mirrors to perform spatial sorting of OAM modes.

2.5 Implementation of unitary matrices by involving Internal modes

In order to reduce the number of beam splitting operations, Dhand et. al. proposed a new algorithm which uses internal DOFs of photons as well for unitary realization [Dhand 15]. This is in contrast to using only the spatial DOFs as proposed by the methods discussed in the Section 2.3. The internal DOFs of photons may include polarization, OAM or time. The main component of their scheme is the Cosine-Sine Decomposition (CSD) algorithm, which is based on the well known Singular Value Decomposition (SVD).

Theorem:

Any arbitrary discrete unitary matrix, say U, of dimensions $(m+n)\times(m+n)$ can be expressed as a product of three matrices,

$$U_{m+n} = \left[\begin{array}{c|c} L_m & 0 \\ \hline 0 & L_n' \end{array}\right] (S_{2m} \oplus \mathbb{1}_{n-m}) \left[\begin{array}{c|c} R_m^\dagger & 0 \\ \hline 0 & R_n'^\dagger \end{array}\right]. \tag{2.33}$$

where L_m, $L_n^{'}$, $R_m^{\dagger}$ and $R_n^{'\dagger}$ are all unitary matrices and S_{2m} is a cosine-sine matrix of the form,

$$S_{2m} = \left[\begin{array}{ccc|ccc} \cos\theta_1 & & & \sin\theta_1 & & \\ & \ddots & & & \ddots & \\ & & \cos\theta_m & & & \sin\theta_m \\ \hline -\sin\theta_1 & & & \cos\theta_1 & & \\ & \ddots & & & \ddots & \\ & & -\sin\theta_m & & & \cos\theta_m \end{array}\right]. \tag{2.34}$$

Proof:

U can be expressed as a block matrix of the form

$$U_{m+n} = \left[\begin{array}{c|c} A & B \\ \hline C & D \end{array}\right]_{2\times 2}, \tag{2.35}$$

where A, B, C, and D are $m \times m$, $m \times n$, $n \times m$, and $n \times n$ dimensional complex matrices respectively. It is well known that the SVD of a complex matrix X of dimensions $m \times n$ is

$$X = M\xi_X V^{\dagger}, \tag{2.36}$$

where M and V are $m \times m$ and $n \times n$ unitary matrices with columns corresponding to eigenvectors of $XX^{\dagger}$ and $X^{\dagger}X$ respectively, and ξ_X is a positive real diagonal matrix. The columns of M and V are also referred to as left-singular vectors and right-singular vectors which diagonalize X.

Since U is unitary,

$$UU^{\dagger} = \mathbb{1}_{m+n} = \left[\begin{array}{c|c} AA^{\dagger} + BB^{\dagger} & AC^{\dagger} + BD^{\dagger} \\ \hline CA^{\dagger} + DB^{\dagger} & CC^{\dagger} + DD^{\dagger} \end{array}\right], \tag{2.37}$$

and,

$$U^{\dagger}U = \mathbb{1}_{m+n} = \left[\begin{array}{c|c} A^{\dagger}A + C^{\dagger}C & A^{\dagger}B + C^{\dagger}D \\ \hline B^{\dagger}A + D^{\dagger}C & B^{\dagger}B + D^{\dagger}D \end{array}\right]. \tag{2.38}$$

Here, $\mathbb{1}_{m+n}$ is the $m+n$-dimensional identity matrix. Comparing the block diagonal identity matrix with the RHS of Eq. 2.37, we get

$$\begin{aligned} AA^{\dagger} + BB^{\dagger} &= \mathbb{1}_m, \\ CC^{\dagger} + DD^{\dagger} &= \mathbb{1}_n. \end{aligned} \tag{2.39}$$

Note that $(AA^{\dagger})^{\dagger} = AA^{\dagger}$, implying that $AA^{\dagger}$ is a normal matrix. This holds true for $BB^{\dagger}$, $CC^{\dagger}$ and $DD^{\dagger}$ as well. Now, multiplying the two equations by $BB^{\dagger}$ and $DD^{\dagger}$

respectively from right as well as left yields

$$\begin{aligned} AA^\dagger BB^\dagger + BB^\dagger BB^\dagger = BB^\dagger, \\ BB^\dagger AA^\dagger + BB^\dagger BB^\dagger = BB^\dagger, \end{aligned} \tag{2.40}$$

and,

$$\begin{aligned} CC^\dagger DD^\dagger + DD^\dagger DD^\dagger = DD^\dagger, \\ DD^\dagger CC^\dagger + DD^\dagger DD^\dagger = DD^\dagger. \end{aligned} \tag{2.41}$$

Subtracting equations in Eq.2.40 and Eq. 2.41, we see that

$$\begin{aligned} [AA^\dagger, BB^\dagger] = 0, \\ [CC^\dagger, DD^\dagger] = 0, \end{aligned} \tag{2.42}$$

which means that $AA^\dagger$ and $CC^\dagger$ commutes with $BB^\dagger$ and $DD^\dagger$ respectively. This suggests that the matrices (A, B) and (C, D) have the same set of left-singular vectors, denoted by matrices L_m and $L_n^{'}$ respectively, upto a defined phase value. Now, we compare the block diagonal identity matrix with the RHS of Eq. 2.38, to get

$$\begin{aligned} A^\dagger A + C^\dagger C = \mathbb{1}_m, \\ B^\dagger B + D^\dagger D = \mathbb{1}_n. \end{aligned} \tag{2.43}$$

A similar procedure as in Eqs. (2.39-2.41) yields

$$\begin{aligned} [A^\dagger A, C^\dagger C] = 0, \\ [B^\dagger B, D^\dagger D] = 0. \end{aligned} \tag{2.44}$$

This shows that the matrices (A, C) and (B, D) have the same set of right-singular vectors, denoted by matrices R_m and $R_n^{'}$ respectively, upto a defined phase value. Now, performing SVD (Eq. 2.36) of unitary matrices A and D yields,

$$A = L_m \xi_A R_m^\dagger, \tag{2.45}$$

$$D = L_n^{'} \xi_D R_n^{'\dagger}. \tag{2.46}$$

Here, ξ_A and ξ_D are real positive matrices, as seen in Eq. 2.36. The matrices L_m, $L_n^{'}$, $R_m^\dagger$ and $R_n^{'\dagger}$ also diagonalize B and C, so that

$$B = L_m \xi_B R_n^{'\dagger}, \tag{2.47}$$

$$C = L_n^{'} \xi_C R_m^\dagger, \tag{2.48}$$

However, their corresponding singular value matrices ξ_B and ξ_C may not be positive real matrices in general, and may contain complex phases. As U is unitary, ξ_B and ξ_C can be expressed as

$$\xi_B = \Phi|\xi_B|, \tag{2.49}$$

$$\xi_C = -|\xi_C|\Phi^\dagger, \tag{2.50}$$

where Φ is a complex phase and $|\xi_B|$, $|\xi_C|$ are the real magnitudes of ξ_B and ξ_C respectively. Eqs. (2.45-2.50) can be expressed in the 2×2 block matrix form to get

$$U_{m+n} = \left[\begin{array}{c|c} L_m & 0 \\ \hline 0 & L_n^{'} \end{array}\right] \left[\begin{array}{c|c} \xi_A & \Phi|\xi_B| \\ \hline -|\xi_C|\Phi^\dagger & \xi_D \end{array}\right] \left[\begin{array}{c|c} R_m^\dagger & 0 \\ \hline 0 & R_n^{'\dagger} \end{array}\right]. \tag{2.51}$$

The phase Φ can be absorbed into the unitary matrices L_m and R_m such that

$$U_{m+n} = \left[\begin{array}{c|c} L_m\Phi & 0 \\ \hline 0 & L_n^{'} \end{array}\right] \left[\begin{array}{c|c} \xi_A & |\xi_B| \\ \hline -|\xi_C| & \xi_D \end{array}\right] \left[\begin{array}{c|c} (R_m\Phi)^\dagger & 0 \\ \hline 0 & R_n^{'\dagger} \end{array}\right]. \tag{2.52}$$

Let us define

$$\Lambda_{m+n} = \left[\begin{array}{c|c} \xi_A & |\xi_B| \\ \hline -|\xi_C| & \xi_D \end{array}\right]. \tag{2.53}$$

It can be easily inferred from Eq. 2.52 that Λ_{m+n} is an orthogonal matrix. Note that any orthogonal square matrix of dimensions 2 can be expressed as a rotation matrix (similar to Eq.2.6), which can be associated with Λ_{m+n} as

$$\Lambda_k = \begin{bmatrix} \cos\theta_k & \sin\theta_k \\ -\sin\theta_k & \cos\theta_k \end{bmatrix}. \tag{2.54}$$

Orthogonality of Λ_{m+n} means that any two columns or rows of Λ_{m+n} are orthogonal to each other. This means that the elements of Λ_{m+n} in the indices (k,k), $(k,k+m)$, $(k+m,k)$ and $(k+m,k+m)$ can be replaced by corresponding elements from Eq. 2.54. This generates a $2m$-dimensional real orthogonal square matrix of the form

$$S_{2m} = \left[\begin{array}{ccc|ccc} \cos\theta_1 & & & \sin\theta_1 & & \\ & \ddots & & & \ddots & \\ & & \cos\theta_m & & & \sin\theta_m \\ \hline -\sin\theta_1 & & & \cos\theta_1 & & \\ & \ddots & & & \ddots & \\ & & -\sin\theta_m & & & \cos\theta_m \end{array}\right]. \tag{2.55}$$

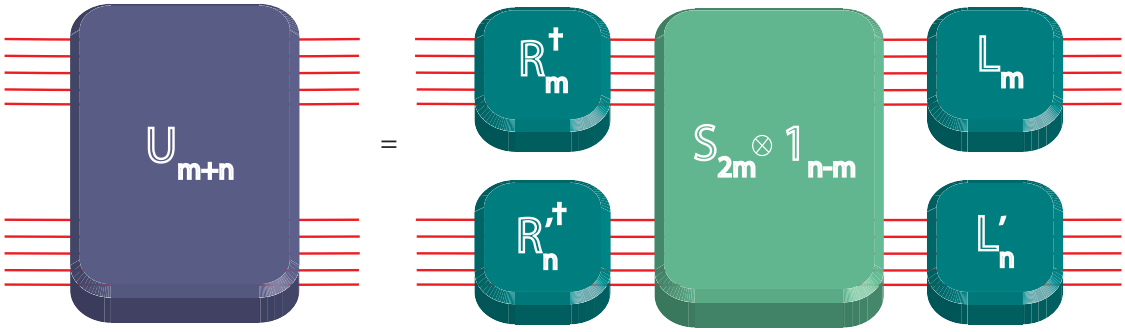

Figure 2.7: *Cosine-Sine Decomposition*: The action of the desired unitary matrix is equivalent to a sequence of three operations. While including the internal modes, this can be interpreted as: A unitary operation acting on the spatial-internal subspace of m and n spatial modes respectively, followed by an operation on all the spatial modes of the photon. The sequence ends with another set of unitary operations on the spatial-internal subspace of the photon alone. Note that actual arrangement of experimental setup is shown here.

In the remaining $n - m$ dimensions, an identity matrix is embedded so that the orthogonality condition of Λ_{m+n} is satisfied. Hence, Eq. 2.52 can be re-expressed as

$$U_{m+n} = \left[\begin{array}{c|c} L_m & 0 \\ \hline 0 & L'_n \end{array}\right] (S_{2m} \oplus \mathbb{1}_{n-m}) \left[\begin{array}{c|c} R_m^\dagger & 0 \\ \hline 0 & R_n'^\dagger \end{array}\right]. \tag{2.56}$$

This concludes the proof for CSD.

This method can be employed to cater in for internal DOFs of light. For that, we inherently assume that the internal degrees of freedom in one spatial mode does not interact with the same in other spatial modes. So, the combined Hilbert space corresponding to QFT operation can be defined as,

$$\mathcal{H} = \mathcal{H}_s \otimes \mathcal{H}_i, \tag{2.57}$$

where $\mathcal{H}_s$ corresponds to the spatial Hilbert space with basis vectors $\{|s_j\rangle\}$ ($j \in \{1, \ldots, n_s\}$) and $\mathcal{H}_i$ corresponds to the Internal Hilbert space with basis vectors $\{|i_k\rangle\}$ ($k \in \{1, \ldots, n_i\}$). $\mathcal{H}_i$ can be further expressed as a direct sum of commuting internal DOF's like polarization and OAM modes, which gives flexibility for the experimentalist to choose the modes according to available resources. The combined basis of the total Hilbert space can be represented as

$$|h_{jk}\rangle = |s_j\rangle \otimes |i_k\rangle\,. \tag{2.58}$$

Choosing the basis for representing the CSD generated matrices let's us identify the

subspace in which optical transformation is to be performed. Now, we see the algorithm developed by Dhand *et al.*, which is as follows

1. The algorithm takes as input the $n_s n_i$-dimensional unitary matrix $U_{n_s n_i}$.

2. Fixing $m = n_i$ and $n = (n_s - 1)n_i$, CSD is performed to get

$$U_{n_s n_i} = \left[\begin{array}{c|c} L_{n_i} & 0 \\ \hline 0 & L^{'}_{(n_s-1)n_i} \end{array}\right] (S_{2n_i} \oplus \mathbb{1}_{(n_s-2)n_i}) \left[\begin{array}{c|c} R^{\dagger}_{n_i} & 0 \\ \hline 0 & R^{'\dagger}_{(n_s-1)n_i} \end{array}\right]. \tag{2.59}$$

   Here, L_{n_i} and $R^{\dagger}_{n_i}$ are unitary matrices acting on a single spatial mode and n_i internal modes. Similarly, $L^{'}_{(n_s-1)n_i}$ and $R^{'\dagger}_{(n_s-1)n_i}$ are unitary matrices acting on $(n_s - 1)$ spatial modes and n_i internal modes. S_{2n_i} acts on the first two spatial modes and the n_i internal modes in each of the spatial modes.

3. In the next iteration, CSD is applied to $L^{'}_{(n_s-1)n_i}$ so that

$$L^{'}_{(n_s-1)n_i} = \left[\begin{array}{c|c} L_{n_i} & 0 \\ \hline 0 & L^{'}_{(n_s-2)n_i} \end{array}\right] (S_{2n_i} \oplus \mathbb{1}_{(n_s-3)n_i}) \left[\begin{array}{c|c} R^{\dagger}_{n_i} & 0 \\ \hline 0 & R^{'\dagger}_{(n_s-2)n_i} \end{array}\right]. \tag{2.60}$$

   Since $R^{'\dagger}_{(n_s-2)n_i}$ commutes with $R^{'\dagger}_{(n_s-1)n_i}$, it can be absorbed in $R^{'\dagger}_{(n_s-1)n_i}$.

4. Iterations are carried out until the dimensions of $L^{'}$ matrix becomes n_i, so that it is affecting only on the internal modes of the last available spatial mode. At this point, $R^{'\dagger}$ matrices would be multiplied together to form a $(n_s-1)n_i$-dimensional unitary matrix,

$$U_{(n_s-1)n_i} = \prod_{k=0}^{n_s-2} R^{'\dagger}_{(n_s-1-k)n_i}. \tag{2.61}$$

5. Steps 1-4 are repeated with input unitary matrix $U_{(n_s-1)n_i}$.

Comparing the form of S_{2n_i} in Eq. 2.55 to that of Eq. 2.6, we can devise that

$$S_{2n_i} = (B \otimes \mathbb{1}_{n_i})(P_{n_i} \oplus P^{\dagger}_{n_i})(B^{\dagger} \otimes \mathbb{1}_{n_i}), \tag{2.62}$$

where B is a balanced beam splitter of the form in Eq. 2.4, and

$$P_{n_i} = \begin{bmatrix} e^{i\theta_1} & & & \\ & e^{i\theta_2} & & \\ & & \ddots & \\ & & & e^{i\theta_{n_i}} \end{bmatrix}. \tag{2.63}$$

This decomposition scheme only requires $(n_s(n_s - 1))$ beam splitters, compared to

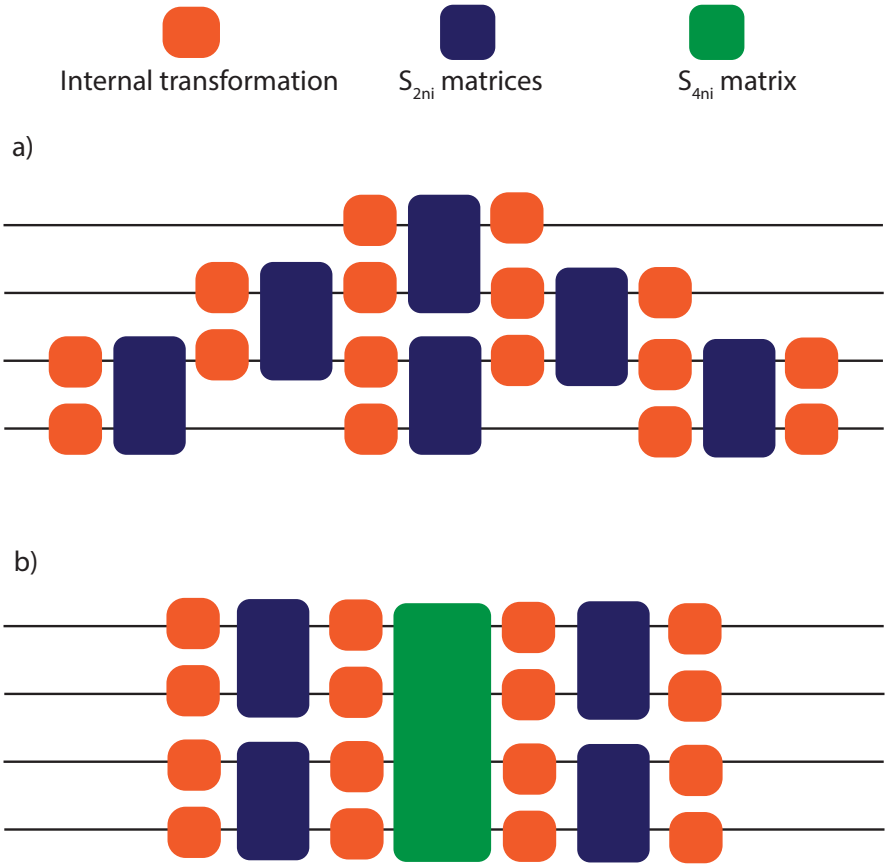

Figure 2.8: *Internal Spatial decomposition*: Two methods by which internal modes can be included in the decomposition algorithm. Here, $n_s = 4$. a) Dhand *et al.* scheme generates a triangular array of six beam splitting operations (S_{2n_i} matrices) and $n_s^2 = 16$ internal operations. Note that each blue box contains two additional internal operations in the form of P_{n_i} and $P_{n_i}^\dagger$. b) Modifying the choice of m and n generates a rectangular array of six beam splitting operations. The green box contains two beam splitting operations (S_{4n_i} matrix) and four internal operations. The total number of internal and spatial transformations remains the same.

$n_s n_i(n_s n_i - 1)/2$ beam splitters required by schemes employing only spatial modes (see Section 2.3). This means the number of beam splitters were reduced by a factor of $n_i^2/2$, when internal modes were employed along with spatial modes for decomposition. However, the total number of internal transformation elements required for realizing the matrix goes up by a factor of two by this approach [Dhand 15].

This algorithm generates a triangular array of beam splitters for the spatial transformation part, similar to Reck's scheme (see Fig. 2.8.a). However, it can be adapted to Clements' method simply by choosing $m = floor(n_s/2)n_i = \lfloor n_s/2 \rfloor n_i$

and $n = ceil(n_s/2)n_i = \lceil n_s/2 \rceil n_i$ when performing CSD. This results in

$$U_{n_s n_i} = \left[\begin{array}{c|c} L_{(\lfloor n_s/2 \rfloor)n_i} & 0 \\ \hline 0 & L'_{(\lceil n_s/2 \rceil)n_i} \end{array}\right] (S_{2\left(\lfloor \frac{n_s}{2} \rfloor\right)n_i} \oplus \mathbb{1}_{\left(\lceil \frac{n_s}{2} \rceil - \lfloor \frac{n_s}{2} \rfloor\right)n_i}) \left[\begin{array}{c|c} R^{\dagger}_{(\lfloor n_s/2 \rfloor)n_i} & 0 \\ \hline 0 & R'^{\dagger}_{(\lceil n_s/2 \rceil)n_i} \end{array}\right]. \tag{2.64}$$

In the next iteration, CSD is performed on the matrices $L_{(\lfloor n_s/2 \rfloor)n_i}$, $L'_{(\lceil n_s/2 \rceil)n_i}$, $R^{\dagger}_{(\lfloor n_s/2 \rfloor)n_i}$ and $R'^{\dagger}_{(\lceil n_s/2 \rceil)n_i}$. This is carried out recursively until all the L and R matrices are of dimension n_i.

This method generates a rectangular array of beam splitters (see Fig. 2.8.b), similar to that produced in Clements' scheme. Although, this approach doesn't change the total number of components or the number of beam splitters required for realization, it helps in improving the fidelity of the circuit (as discussed in Section 2.3).

2.6 Adapting Torma *et al.* QFT factorization to include internal modes

Torma *et al.* proposed an algorithm that makes use of a general Cooley-Tukey algorithm to separate the action of a $N = N_1 N_2$-dimensional QFT into action of several N_1-dimensional and N_2-dimensional QFT matrices [Törmä 96]. They considered the specific case of using spatial modes to implement the desired QFT operation. When $N = 2^n$ for positive integer values of n, their scheme required only $\mathcal{O}(Nlog_2 N)$ number of beam splitters.

In this section, we adapt Torma's decomposition scheme to include the internal DOFs of light as well. We derive the general decomposition algorithm which uses internal modes of light, and discuss about the permutation matrices involved in the decomposition in point of view of the internal modes as well.

2.6.1 Deriving the general decomposition

Cooley-Tukey algorithm is a recursive algorithm used to compute discrete fourier transform of a given function. For N-dimensional set of annihilation operators $\{\hat{a}_j\}$, where $j = 0, 1, 2, \ldots, N-1$, the QFT is given as

$$\hat{b}_k = \sum_{j=0}^{N-1} \omega^{kj} \hat{a}_j, \tag{2.65}$$

where $\omega = \exp(i2\pi/N)$, and $\hat{b}_k$ (where $k = 0, 1, 2, ...N-1$) is the output annihilation operators upon performing QFT. When applied for a two-point case, Cooley-Tukey algorithm exploits the symmetry of the complex exponential in the QFT to express

N-dimensional transformations as a combination of two $(N/2)$-dimensional transformations acting on the even and odd indices respectively [Cooley 65], so that

$$\begin{aligned}\hat{b}_k &= \frac{1}{\sqrt{N}}\left(\sum_{j=0}^{\frac{N}{2}-1}\omega^{k(2j)}\hat{a}_{2j} + \sum_{j=0}^{\frac{N}{2}-1}\omega^{k(2j+1)}\hat{a}_{2j+1}\right)\\ &= \frac{1}{\sqrt{N}}\sum_{j=0}^{\frac{N}{2}-1}\omega^{k(2j)}\hat{a}_{2j} + \frac{\omega^k}{\sqrt{N}}\sum_{j=0}^{\frac{N}{2}-1}\omega^{k(2j)}\hat{a}_{2j+1}\\ &= A_{even} + \omega^k A_{odd},\end{aligned} \tag{2.66}$$

with A_{even} and A_{odd} being the QFT of even and odd indices of $\{\hat{a}_j\}_{j=0}^{N-1}$ respectively. Due to the recursive nature of the algorithm, this is continued until we are left with the lowest dimensional transformations required to act as the desired N-dimensional QFT. In matrix notation, Eq.(2.65) assumes the form

$$\boldsymbol{b} = F_N \boldsymbol{a}, \tag{2.67}$$

where $\boldsymbol{b}$ and $\boldsymbol{a}$ are N dimensional vectors corresponding to $\{\hat{b}_k\}_{k=0}^{N-1}$ and $\{\hat{a}_j\}_{j=0}^{N-1}$, and F_N is a $N \times N$ dimensional matrix given by

$$F_N = \frac{1}{\sqrt{N}}\begin{bmatrix} 1 & 1 & 1 & \cdots & 1 \\ 1 & \omega & \omega^2 & \cdots & \omega^{N-1} \\ 1 & \omega^2 & \omega^4 & \cdots & \omega^{2(N-1)} \\ \vdots & \vdots & \vdots & \ddots & \vdots \\ 1 & \omega^{(N-1)} & \omega^{2(N-1)} & \cdots & \omega^{(N-1)(N-1)} \end{bmatrix}. \tag{2.68}$$

Here, F_N is the matrix representation of the QFT transformation. The matrix F_N is a symmetric unitary matrix and has a degenerate set of eigenvalues $(1, i, -1, -i)$. This matrix can be decomposed into a set of smaller matrices which are easily realizable using various schemes of decomposition. For simplicity, we omit the normalization factor of $1/\sqrt{N}$.

$$F_N = \left[\begin{array}{c|c} \mathbb{1}_{N/2} & D_{N/2} \\ \hline \mathbb{1}_{N/2} & \omega^{N/2} D_{N/2} \end{array}\right]\left[\begin{array}{c|c} F_{N/2} & 0 \\ \hline 0 & F_{N/2} \end{array}\right] P_N, \tag{2.69}$$

Note that $\omega^{N/2} = -1$. Now, the first matrix on the RHS of Eq.2.69 can be expressed as a combination of matrices generated through CSD,

$$\begin{aligned}F_N = &\left[\begin{array}{c|c} \mathbb{1}_{N/2} & 0 \\ \hline 0 & -\mathbb{1}_{N/2} \end{array}\right]\left[\begin{array}{c|c} \mathbb{1}_{N/2} & \mathbb{1}_{N/2} \\ \hline -\mathbb{1}_{N/2} & \mathbb{1}_{N/2} \end{array}\right]\\ &\times\left[\begin{array}{c|c} \mathbb{1}_{N/2} & 0 \\ \hline 0 & D_{N/2} \end{array}\right]\left[\begin{array}{c|c} F_{N/2} & 0 \\ \hline 0 & F_{N/2} \end{array}\right] P_N.\end{aligned} \tag{2.70}$$

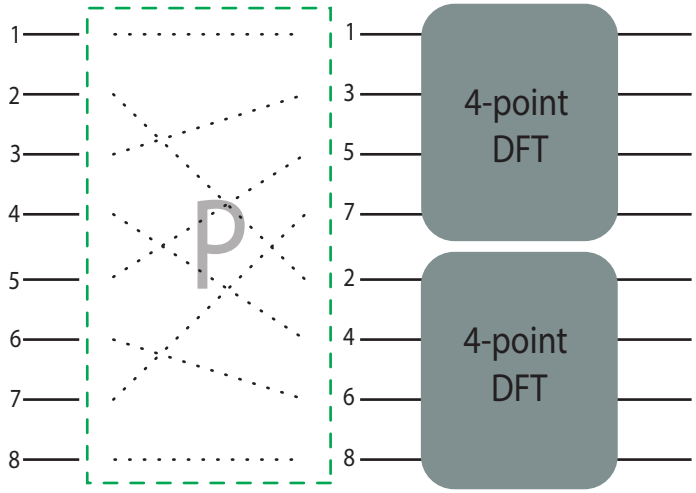

Figure 2.9: *Action of Permutation matrix*: Shown here is the operation of an eight-dimensional permutation matrix for the case of a two-point discrete Fourier transform based on Cooley-Tukey algorithm. For simplicity, we consider only the spatial modes. Applying the permutation breaks the eight-dimensional QFT into equivalent four-dimensional QFT operations.

Multiplying the first two matrices in the RHS of Eq. 2.70,

$$F_N = \left[\begin{array}{c|c} \mathbb{1}_{N/2} & \mathbb{1}_{N/2} \\ \hline \mathbb{1}_{N/2} & -\mathbb{1}_{N/2} \end{array}\right] \left[\begin{array}{c|c} \mathbb{1}_{N/2} & 0 \\ \hline 0 & D_{N/2} \end{array}\right] \left[\begin{array}{c|c} F_{N/2} & 0 \\ \hline 0 & F_{N/2} \end{array}\right] P_N. \tag{2.71}$$

The leftmost matrix in the RHS of Eq.2.71 corresponds to a QFT operation on a two-dimensional subspace, which stems from the fact that we have used a regular 2-point Cooley-Tukey algorithm to split the N-dimensional QFT into $(N/2)$-dimensional QFTs.

Let us consider the case where internal modes are included. Now, $N = n_s n_i$, where n_s represents number of spatial modes and n_i represents number of internal modes. Similar to the 2-point QFT case, we can represent the $n_s n_i$-dimensional QFT by splitting into n_s components as

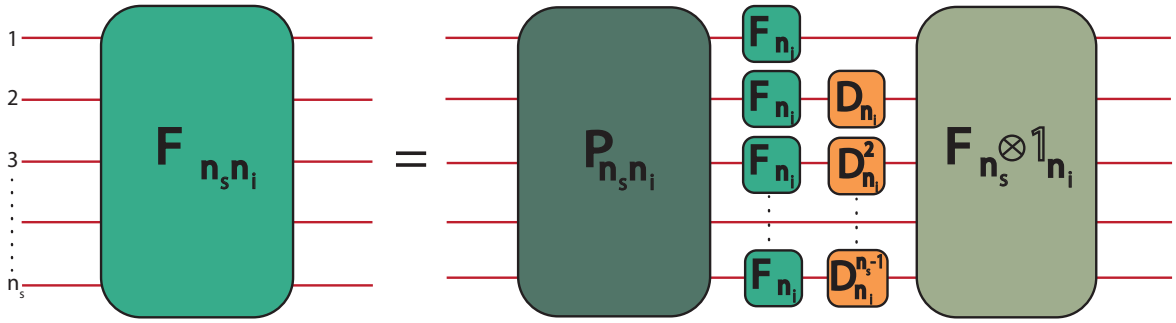

Figure 2.10: *Visualization of the general decomposition algorithm*: QFT is implemented in steps as shown in the figure. First, a permutation is done on the input modes, followed by QFT operations on the internal subspace of the photon, in every spatial mode. Then, a set of diagonal unitary operations takes place leaving the first spatial mode unaffected. Finally, a QFT operation on the spatial degree of freedom is performed. Note that this is the actual order in which experimental setup is arranged.

$$\begin{aligned}\hat{b}_k &= \sum_{j=0}^{n_i-1} \omega^{k(n_s j)} \hat{a}_{n_s j} + \sum_{j=0}^{n_i-1} \omega^{k(n_s j+1)} \hat{a}_{n_s j+1} \\ &\quad + \cdots + \sum_{j=0}^{n_i-1} \omega^{k(n_s j+n_s-1)} \hat{a}_{n_s j+n_s-1} \\ &= \sum_{j=0}^{n_i-1} \omega^{k(n_s j)} \hat{a}_{n_s j} + \omega^k \sum_{j=0}^{n_i-1} \omega^{k(n_s j)} \hat{a}_{n_s j+1} \\ &\quad + \cdots + \omega^{k(n_s-1)} \sum_{j=0}^{n_i-1} \omega^{k(n_s j)} \hat{a}_{n_s j+n_s-1},\end{aligned} \tag{2.72}$$

for $k = 0, 1, \ldots, n_s n_i - 1$. We have permuted the modes in such a way that n_s number of n_i-dimensional QFT operations are performed to get back the original QFT. The corresponding matrix form is,

$$\boldsymbol{b} = \begin{bmatrix} 1 & 1 & \cdots & 1 \\ 1 & \omega^{n_s} & \cdots & \omega^{(n_s-1)+n_s(n_i-1)} \\ 1 & \omega^{2n_s} & \cdots & \omega^{2((n_s-1)+n_s(n_i-1))} \\ \vdots & \vdots & \ddots & \vdots \\ 1 & \omega^{(n_s n_i-1)n_s} & \cdots & \omega^{(n_s n_i-1)((n_s-1)+n_s(n_i-1))} \end{bmatrix} \boldsymbol{a} \tag{2.73}$$

This matrix can be partitioned on the basis of the summation form in Eq.2.72, and we see that it is essentially made up of n_s^2 number of n_i-dimensional QFT operations. Hence, the transformation in Eq.2.73 can be decomposed as

$$\tilde{F}_{n_s n_i} = \tilde{F} \left[\begin{array}{c|c|c|c} F_{n_i} & & & \\ \hline & F_{n_i} & & \\ \hline & & \ddots & \\ \hline & & & F_{n_i} \end{array}\right], \tag{2.74}$$

where $\tilde{F}_{n_s n_i}$ denotes the original QFT matrix after permutation,

$$F_{n_i} = \begin{bmatrix} 1 & 1 & \cdots & 1 \\ 1 & \omega^{n_s} & \cdots & \omega^{n_s(n_i-1)} \\ \vdots & \vdots & \ddots & \vdots \\ 1 & \omega^{(n_i-1)n_s} & \cdots & \omega^{n_s(n_i-1)^2} \end{bmatrix}, \tag{2.75}$$

and

$$\tilde{F} = \begin{bmatrix} \mathbb{1}_{n_i} & D_{n_i} & \cdots & D_{n_i}^{n_s-1} \\ \mathbb{1}_{n_i} & \omega^{n_i} D_{n_i} & \cdots & \omega^{n_i(n_s-1)} D_{n_i}^{n_s-1} \\ \vdots & \vdots & \ddots & \vdots \\ \mathbb{1}_{n_i} & \omega^{n_i(n_s-1)} D_{n_i} & \cdots & \omega^{n_i(n_s-1)^2} D_{n_i}^{n_s-1} \end{bmatrix}. \tag{2.76}$$

Here, D_{n_i} is a diagonal matrix with complex entries $(1, \omega, \omega^2, \ldots, \omega^{n_i-1})$. Now, CSD can be applied to $\tilde{F}$ to get

$$\tilde{F} = \begin{bmatrix} \mathbb{1}_{n_i} & \mathbb{1}_{n_i} & \cdots & \mathbb{1}_{n_i} \\ \mathbb{1}_{n_i} & \omega^{n_i}\mathbb{1}_{n_i} & \cdots & \omega^{n_i(n_s-1)}\mathbb{1}_{n_i} \\ \vdots & \vdots & \ddots & \vdots \\ \mathbb{1}_{n_i} & \omega^{n_i(n_s-1)}\mathbb{1}_{n_i} & \cdots & \omega^{n_i(n_s-1)^2}\mathbb{1}_{n_i} \end{bmatrix} \begin{bmatrix} \mathbb{1}_{n_i} & & & \\ & D_{n_i} & & \\ & & \ddots & \\ & & & D_{n_i}^{n_s-1} \end{bmatrix}. \tag{2.77}$$

From this, we see that any $n_s n_i$-dimensional QFT can be split into n_s-dimensional and n_i-dimensional QFTs by exploiting the structure of the permutation matrix, which is responsible for splitting the total summation form into smaller summation forms over desired indices. Therefore, $F_{n_s n_i}$ can be decomposed as (Fig.2.10),

$$F_{n_s n_i} = (F_{n_s} \otimes \mathbb{1}_{n_i})(\mathbb{1}_{n_i} \oplus D_{n_i} \oplus \ldots \oplus D_{n_i}^{n_s-1})(\mathbb{1}_{n_s} \otimes F_{n_i}) P_{n_s n_i}, \tag{2.78}$$

with F_{n_s} being an operation on the spatial modes and F_{n_i} being an operation on the internal modes, and $P_{n_s n_i}$ is a permutation matrix obtained by rearranging the columns of $\mathbb{1}_{n_s n_i}$ in the specific order given by $(1 : n_s : N, 2 : n_s : N, \ldots, n_s : n_s : N)$, and then taking its transpose conjugate.

F_{n_s} can be realized using a combination of $n_s(n_s-1)/2$ beam splitters and $n_s(n_s+1)/2$ phase shifters [Reck 94, Clements 16]. Since this is a recursive algorithm, F_{n_i} can be

further decomposed in the second iteration of the algorithm as

$$F_{n_p n_o} = (F_{n_p} \otimes \mathbb{1}_{n_o})(\mathbb{1}_{n_o} \oplus D_{n_o} \oplus \ldots \oplus D_{n_o}^{n_p-1})(\mathbb{1}_{n_p} \otimes F_{n_o})P_{n_p n_o}. \tag{2.79}$$

Here, F_{n_p} is a QFT operation on polarization modes, which can be realized through combinations of waveplates [Simon 89] and phase shifters. F_{n_o} is an operation on OAM modes, which can be realized upto three dimensions using cylindrical lenses, Dove prisms, lenses and SLMs [Arrizón 07] (as discussed in Section 3.3.1). The iterations are continued until the lowest implementable dimensions are achieved, which may be F_2 or F_3.

2.6.2 Permutation involving internal modes

The structure of the permutation matrix depends on the value of n_s. Here, $1 : n_s : N$ corresponds to a syntax of the form $initial : step\_size : final$, which is used to specify the order in which the columns of the identity matrix is to be permuted as per the algorithm. It denotes the set of numbers generated by adding the value n_s to the initial value specified at the left, upto the final value specified at the right. So, $1 : 2 : 8$ would generate the set $(1, 3, 5, 7)$, and $2 : 2 : 8$ would generate the set $(2, 4, 6, 8)$. After this, the operation denoted by $(,)$ concatenates these sets together to specify that the columns of the identity matrix should be rearranged in the order $(1, 3, 5, 7, 2, 4, 6, 8)$.

A general scheme for realization of arbitrary dimensional permutation operations involving spatial and internal modes is yet to be achieved. This is due to the fact that higher dimensional permutation matrices have associated degeneracy, which implies that a set of decomposition matrices can exist for representing a single permutation. Finding the optimal implementable decomposition from this set is still a challenge. However, we discuss implementations of specific cases of permutation matrices in Chapter 3.

2.7 Schwinger's representation

In 1965, Schwinger showed that two independent harmonic oscillators can be used to construct the Lie algebra related to orbital angular momentum. Let $(\hat{a}_1, \hat{a}_1^\dagger)$ and $(\hat{a}_2, \hat{a}_2^\dagger)$ denote the creation and annihilation operators of the two independent harmonic oscillators respectively. These operators abide by the fundamental commutation relation $[\hat{a}_i, \hat{a}_i^\dagger] = 1$ and the number operators related to these oscillators can be written as $N_i = \hat{a}_i^\dagger \hat{a}_i$, for $i = 1, 2$. Now, we can define a set of angular momentum

operators in terms of $(\hat{a}_1, \hat{a}_1^\dagger; \hat{a}_2, \hat{a}_2^\dagger)$.

$$\begin{aligned}\hat{J}_1 &= \frac{\hbar}{2}(\hat{a}_1^\dagger \hat{a}_1 - \hat{a}_2^\dagger \hat{a}_2),\\ \hat{J}_2 &= \frac{\hbar}{2}(\hat{a}_1^\dagger \hat{a}_2 + \hat{a}_2^\dagger \hat{a}_1),\\ \hat{J}_3 &= \frac{\hbar}{2}(\hat{a}_2^\dagger \hat{a}_1 - \hat{a}_1^\dagger \hat{a}_2).\end{aligned} \tag{2.80}$$

These three operators satisfy the Lie algebra for angular momentum given by,

$$[\hat{J}_j, \hat{J}_k] = i\hbar\epsilon_{jkl}\hat{J}_l. \tag{2.81}$$

Now, we can define the operator

$$\hat{J}_0 = \frac{\hbar}{2}(\hat{a}_1^\dagger \hat{a}_1 + \hat{a}_2^\dagger \hat{a}_2), \tag{2.82}$$

which satisfies,

$$[\hat{J}_0, \hat{J}_l] = 0, \text{ (for } l = 1, 2, 3). \tag{2.83}$$

This suggests that $\hat{J}_0$ can be paired with any of $\{\hat{J}_i\}_{i=1}^3$ operators to generate a complete set of commuting operators. The simultaneous eigenfunctions of such operators form a complete basis in the Hilbert space. Here, the direct product space of the uncoupled harmonic oscillators yield the orbital angular momentum space and can be denoted as,

$$\mathcal{H} = \mathcal{H}_1 \otimes \mathcal{H}_2, \tag{2.84}$$

where $\mathcal{H}_1$ and $\mathcal{H}_2$ denotes the Hilbert space of the two independent harmonic oscillators and $\mathcal{H}$ denotes the Hilbert space of the angular momentum operators. The states $|n_1, n_2\rangle$ forms the basis for the Hilbert space $\mathcal{H}$. The simultaneous eigenfunctions of the operators $\hat{J}_0$ and $\hat{J}_3$ are the Laguerre-Gaussian (LG) modes. The action of $\hat{J}_0$ and $\hat{J}_3$ on the basis states yield,

$$\begin{aligned}\hat{J}_0 |n_1, n_2\rangle &= \frac{\hbar}{2}(n_1 + n_2) |n_1, n_2\rangle ,\\ \hat{J}_3 |n_1, n_2\rangle &= \frac{\hbar}{2}(n_1 - n_2) |n_1, n_2\rangle .\end{aligned} \tag{2.85}$$

Let us introduce a change of variables $j = (n_1 + n_2)/2$ and $m = (n_1 - n_2)/2$, which results in the following equations,

$$\begin{aligned}\hat{J}_0 |j, m\rangle &= j\hbar |j, m\rangle ,\\ \hat{J}_3 |j, m\rangle &= m\hbar |j, m\rangle .\end{aligned} \tag{2.86}$$

We see that n_1 and n_2 can only take non-negative integer values. This implies that j can only take non-negative half-integer and integer values, and m can take values from $-j$ to j in integer steps [Simon 93].

2.8 Implementation of Schwinger's matrices

The generators that were discussed in Section 2.7 can be used to form matrices with the basis corresponding to the OAM states, in a similar parameterization as in Eq. 2.3. The ability to realize such matrices that are generated using $\{\hat{J}_i\}_{i=1}^3$ is important for the realization of three-dimensional QFT, as discussed in Section 3.3.1.
Consider a paraxial light beam propagating along z direction. This can be expressed as

$$\Psi(x, y, z, t) = \Psi'(x, y, z)e^{i(kz-\omega t)} \tag{2.87}$$

Any unitary operation U would transform a paraxial field as

$$\Phi(x, y, z) = U\Psi'(x, y, z) \tag{2.88}$$

The unitary transformation is generated by the quadratic form of position and momentum operators given by $\hat{x} = x$, $\hat{y} = y$, $\hat{p_x} = -i\partial/\partial x$ and $\hat{p_y} = -i\partial/\partial y$. Various unitary operations can be performed on a light field, of which free propagation through a distance d

$$\mathbf{F}_d = e^{-\frac{id}{2k}(\hat{p_x}^2+\hat{p_y}^2)}, \tag{2.89}$$

and action of a thin lens of focal length f

$$\mathbf{L}_f = e^{-\frac{ik}{2f}(\hat{x}^2+\hat{y}^2)} \tag{2.90}$$

are the most commonly used first order axially symmetric transformations. The matrices corresponding to these transformations belong to the Symplectic group ($Sp(4, \mathbb{R})$) [Sudarshan 85]. Let $\mathbf{S} \in Sp(4, \mathbb{R})$ and $\hat{\eta}$ denote the vector $[\hat{x}, \hat{p_x}, \hat{y}, \hat{p_y}]^T$. Then,

$$U^\dagger(\mathbf{S})\hat{\eta}U(\mathbf{S}) = \mathbf{S}\hat{\eta}, \tag{2.91}$$

where $\mathbf{S}\Sigma\mathbf{S}^T = \Sigma$, and $\Sigma = \Omega \oplus \Omega$. Here,

$$\Omega = \begin{bmatrix} 0 & 1 \\ -1 & 0 \end{bmatrix}. \tag{2.92}$$

Note that $\det(\mathbf{S}) = 1$, which indicates that the input and output refractive indices are preserved. Using Eq. 2.91, the corresponding matrix form of $\mathbf{F}_d$ and $\mathbf{L}_f$ are

$$\mathbb{F}(d) = \begin{bmatrix} F(d) & 0 \\ 0 & F(d) \end{bmatrix}, \qquad \text{where} \quad \mathrm{F(d)} = \begin{bmatrix} 1 & d \\ 0 & 1 \end{bmatrix}, \tag{2.93}$$

$$\mathbb{L}(f) = \begin{bmatrix} L(f) & 0 \\ 0 & L(f) \end{bmatrix}, \qquad \text{where} \quad \mathrm{L(f)} = \begin{bmatrix} 1 & 0 \\ -1/f & 1 \end{bmatrix}. \tag{2.94}$$

For the case of an axially asymmetric transformation, we have thin cylindrical lens of focal length f, which transforms the beam only in a specific direction, and is given by

$$\mathbb{L}_x(f) = \begin{bmatrix} L(f) & 0 \\ 0 & \mathbb{1}_2 \end{bmatrix}, \quad \text{and} \quad \mathbb{L}_{\mathrm{y}}(\mathrm{f}) = \begin{bmatrix} \mathbb{1}_2 & 0 \\ 0 & L(f) \end{bmatrix}. \tag{2.95}$$

Here, $\mathbb{L}_x(f)$ acts only on the vector $[\hat{x}, \hat{p}_x]^T$, and $\mathbb{L}_y(f)$ acts only on the vector $[\hat{y}, \hat{p}_y]^T$. Now, the generators in Eq. 2.80 and Eq. 2.82 can be re-expressed in the position representation as

$$\hat{J}_0 = \frac{1}{4}(\hat{x}^2 + \hat{y}^2 + \hat{p_x}^2 + \hat{p_y}^2) - \frac{1}{2}, \tag{2.96}$$

$$\hat{J}_1 = \frac{1}{4}(\hat{x}^2 - \hat{y}^2 + \hat{p_x}^2 - \hat{p_y}^2), \tag{2.97}$$

$$\hat{J}_2 = \frac{1}{2}(\hat{x}\hat{y} + \hat{p_x}\hat{p_y}), \tag{2.98}$$

$$\hat{J}_3 = \frac{1}{2}(\hat{x}\hat{p_y} - \hat{y}\hat{p_x}), \tag{2.99}$$

Using Eq. 2.91 with $U = e^{i2\theta\hat{J}_l}$ (for $l = 0, 1, 2, 3$), the corresponding matrix formalism of these operators can be found to be

$$\mathbb{J}_0(\theta) = \begin{bmatrix} R(\theta) & 0 \\ 0 & R(\theta) \end{bmatrix}, \tag{2.100}$$

$$\mathbb{J}_1(\theta) = \begin{bmatrix} R(\theta) & 0 \\ 0 & R(-\theta) \end{bmatrix}, \tag{2.101}$$

$$\mathbb{J}_2(\theta) = \begin{bmatrix} \cos\theta\mathbb{1}_2 & -\sin\theta\,\epsilon_1 \\ -\sin\theta\,\epsilon_1 & \cos\theta\mathbb{1}_2 \end{bmatrix}, \tag{2.102}$$

$$\mathbb{J}_3(\theta) = \begin{bmatrix} \cos\theta\mathbb{1}_2 & \sin\theta\mathbb{1}_2 \\ -\sin\theta\mathbb{1}_2 & \cos\theta\mathbb{1}_2 \end{bmatrix}, \tag{2.103}$$

where $R(\theta)$ is a rotation matrix of the form in Eq. 2.10 and

$$\epsilon_1 = \begin{bmatrix} 0 & 1 \\ -1 & 0 \end{bmatrix}. \tag{2.104}$$

It is easy to see that ϵ_1 can be decomposed as

$$\begin{aligned} \epsilon_1 &= F(1)L(1)F(1) \\ &= \begin{bmatrix} 1 & 1 \\ 0 & 1 \end{bmatrix} \begin{bmatrix} 1 & 0 \\ -1 & 1 \end{bmatrix} \begin{bmatrix} 1 & 1 \\ 0 & 1 \end{bmatrix} \\ &= \begin{bmatrix} 1 & 1 \\ 0 & 1 \end{bmatrix} \begin{bmatrix} 1 & 1 \\ -1 & 0 \end{bmatrix} \\ &= \begin{bmatrix} 0 & 1 \\ -1 & 0 \end{bmatrix}. \end{aligned} \tag{2.105}$$

Hence, one convex lens is essential for implementing ϵ_1. Similarly, ϵ_1^{-1} can be decomposed as

$$\epsilon_1^{-1} = F(2)L(1)F(3)L(1)F(2), \tag{2.106}$$

requiring two convex lenses for implementation.

Now, $\mathbb{J}_l(\theta) \in Sp(4, \mathbb{R})$, for $l = 0, 1, 2, 3$. In particular, note that $\mathbb{J}_0(\theta)$ and $\mathbb{J}_1(\theta)$ are in a block diagonal form. Any symplectic matrix of the form $\mathbf{S} = S_1 \oplus S_2$, where $S_1, S_2 \in Sp(2, \mathbb{R})$ (two-dimensional symplectic matrices), can be realized using a maximum of three convex lenses and seven cylindrical lenses with $f > 1$ [Ameen Yasir 17]. To see this result, note that $\mathbf{S}$ can be decomposed as

$$\begin{aligned} \mathbf{S} &= \begin{bmatrix} S_1 & 0 \\ 0 & S_2 \end{bmatrix} \\ &= \begin{bmatrix} -S_1 & 0 \\ 0 & -S_1 \end{bmatrix} \begin{bmatrix} -F(-d) & 0 \\ 0 & -\mathbb{1}_2 \end{bmatrix} \begin{bmatrix} F(d) & 0 \\ 0 & S_1^{-1}S_2 \end{bmatrix} \\ &= (\mathbb{1}_2 \otimes -S_1)(-F(-d) \oplus -\mathbb{1}_2)(F(d) \oplus S_1^{-1}S_2). \end{aligned} \tag{2.107}$$

In general, $-S_1$ in $(\mathbb{1}_2 \otimes -S_1)$ can be represented using a 2×2 matrix of the form

$$-S_1 = \begin{bmatrix} -a & -b \\ -c & -d \end{bmatrix}, \tag{2.108}$$

where a, b, c, d are positive real entries and $ad - bc = 1$. Such a matrix can be decomposed as

$$-S_1 = F\left(\frac{1+a}{c}\right)\epsilon_1^{-1}F(c)\epsilon_1 F\left(\frac{1+d}{c}\right), \tag{2.109}$$

requiring three convex lenses (two from ϵ_1^{-1} and one from ϵ_1) for implementation [Yasir 14]. Now, $(-F(-d) \oplus -\mathbb{1}_2)$ is a unitary operation causing inverse free propagation of the light field in the x direction. This can be decomposed as

$$-(F(-d) \oplus \mathbb{1}_2) = L_x\left(\frac{d}{2}\right) F\left(\frac{d}{4}\right) L_y\left(\frac{d}{4}\right) F\left(\frac{d}{2}\right) L_y\left(\frac{d}{4}\right) F\left(\frac{d}{4}\right) L_x\left(\frac{d}{2}\right), \quad (2.110)$$

requiring four cylindrical lenses for implementing the transformation. Finally, $(F(d) \oplus S_1^{-1}S_2)$ can be expressed as

$$F(d) \oplus S_1^{-1}S_2 = \begin{bmatrix} F(d) & 0 \\ 0 & \mathbb{1}_2 \end{bmatrix} \begin{bmatrix} \mathbb{1}_2 & 0 \\ 0 & S_1^{-1}S_2 \end{bmatrix} \quad (2.111)$$

Here $S_1^{-1}S_2$ is a symplectic matrix realized by not more than three convex lenses, as in Eq.2.109. The entire block $(\mathbb{1}_2 \oplus S_1^{-1}S_2)$ thus corresponds to action of three $L_y(f)$ cylindrical lenses. Also,

$$F(d) \oplus \mathbb{1}_2 = F\left(\frac{d}{3}\right) L_y\left(\frac{d}{9}\right) F\left(\frac{d}{3}\right) L_y\left(\frac{d}{9}\right) F\left(\frac{d}{3}\right) L_y\left(\frac{d}{9}\right). \quad (2.112)$$

Hence, it requires a total of three cylindrical lenses to implement $F(d) \oplus S_1^{-1}S_2$, with d corresponding to the total distance in the cylindrical lens setup. Summing up the components required for implementing $\mathbf{S} = S_1 \oplus S_2$, we see that it requires a maximum of three convex lenses and seven cylindrical lenses to impart the transformation to the paraxial light field.

2.9 Diagonal unitary operation on OAM modes

In 2010, Berkhout *et al.* noted that refractive optical elements can be engineered to perform a log-polar co-ordinate transformation on the incident light field carrying OAM [Berkhout 10]. Such refractive elements transforms the azimuthal component of the input LG beam corresponding to OAM to a transverse position in the output beam. Let this map be between the co-ordinates (x, y) to (u, v). In our case, let (x, y) be mapped to

$$u = -ln\left(\frac{\sqrt{x^2 + y^2}}{b}\right), \quad (2.113)$$

$$v = a\, arctan\left(\frac{y}{x}\right). \quad (2.114)$$

For this co-ordinate mapping, the amplitude of the incoming light field is multiplied

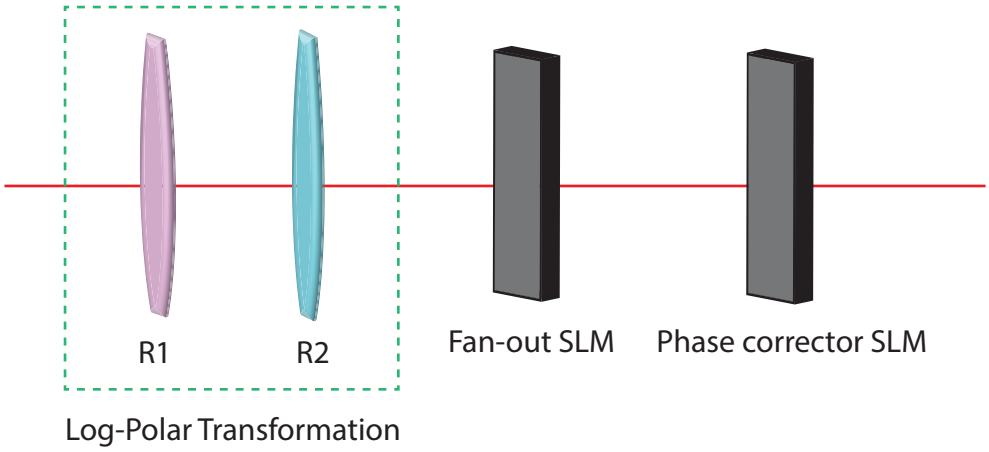

Figure 2.11: *Experimental setup for performing diagonal unitary operation on OAM modes*: R1 and R2 are refractive elements that perform the log-polar co-ordinate mapping. A fan-out SLM performs refractive beam copying to generate well resolved spots of varying OAM values. The following SLM performs the desired phase operation corresponding to the diagonal unitary matrix.

with the phase element

$$\Phi_1(x,y) = \frac{2\pi a}{\lambda f}\left[y\, arctan\left(\frac{y}{x}\right) - x\, ln\left(\frac{\sqrt{x^2+y^2}}{b}\right) + x\right], \tag{2.115}$$

where f is the focal length of the Fourier transforming lens and λ is the wavelength of the incoming beam. a scales the image according to $a = d/2\pi$, where d is the length of the output beam, and b performs a translation in the direction of u. A second phase element, $\Phi_2(u,v)$, is added at the Fourier plane (u,v) for performing phase correction, such that

$$\Phi_2(u,v) = -\frac{2\pi a}{\lambda f} exp\left(-\frac{u}{a}\right) cos\left(\frac{v}{a}\right). \tag{2.116}$$

Berkhout *et al.* used SLMs to fabricate the required phase elements. Later, Mirhosseini *et al.* improved this scheme by using specifically manufactured refractive elements with desired phase structure of $\Phi_1(x,y)$ and $\Phi_2(u,v)$, along with a fan-out copy SLM which performs beam copying. The beam copying step added to the resolution of the output OAM modes, increasing the mode separation efficiency of the entire setup [Mirhosseini 13]. The phase structure of the fan-out copy SLM is given by

$$\Phi_{2N+1}(x) = tan^{-1}\left(\frac{\sum_{k=-N}^{N} \alpha_k sin[(2\pi s/\lambda)kx + \beta_k]}{\sum_{k=-N}^{N} \alpha_k cos[(2\pi s/\lambda)kx + \beta_k]}\right), \tag{2.117}$$

where $2N+1$ is the total number of copies of the beam and s is the angular separation between the number of copies. x denotes the direction in which copying is carried out. α_k and β_k are parameters which can be numerically optimized to generate a

uniformly distributed intensity profile.

We modify this scheme to add one more SLM, which imparts different phase operations on the transverse mapped output beam. This can be used to perform any arbitrary diagonal unitary operation on the OAM modes. After performing the diagonal unitary operation, refractive elements $\Phi_1(x, y)$ and $\Phi_2(u, v)$ are acted in reverse to get back the azimuthal OAM phase. Hence, it requires 6 components to achieve an arbitrary diagonal unitary operation on N OAM modes.

Chapter 3

Optical implementation of QFT using spatial and internal DOFs

We have seen in the previous chapter that various DOFs of light can be used to realize the operation of an arbitrary unitary matrix experimentally. As we have noted earlier, reducing the number of beam splitters required for the unitary matrix realization would be helpful to improve the fidelity of the output state. In this chapter, we use the adapted version of Torma's algorithm for QFT factorization presented in Section 2.6 to understand its effect on the number of beam splitters. The hardest part of this implementation is the realization of permutation matrices involving internal DOFs. We present specific cases of permutation matrices and see how it can be decomposed into smaller permutations in the internal subspace of the photon.

3.1 Four-dimensional QFT

We demonstrate the application of our scheme by starting with the realization of the four-dimensional QFT. The choice of basis is subjective, and for demonstration, we choose two polarizaion modes and two OAM modes. Applying our adaptation of Torma's scheme yields,

$$F_4 = (F_2 \otimes \mathbb{1}_2)(\mathbb{1}_2 \oplus D_2)(\mathbb{1}_2 \otimes F_2)P_4. \tag{3.1}$$

Here, $(F_2 \otimes \mathbb{1}_2)$ is a Hadamard operation on the polarization DOF. From Section 2.2.2, we see that

$$\begin{aligned} H_{\pi/8} &= R(\pi/8)H_0R(-\pi/8) \\ &= H_0R(-\pi/4) \\ &= \frac{i}{\sqrt{2}}\begin{bmatrix} 1 & 1 \\ 1 & -1 \end{bmatrix} \end{aligned} \tag{3.2}$$

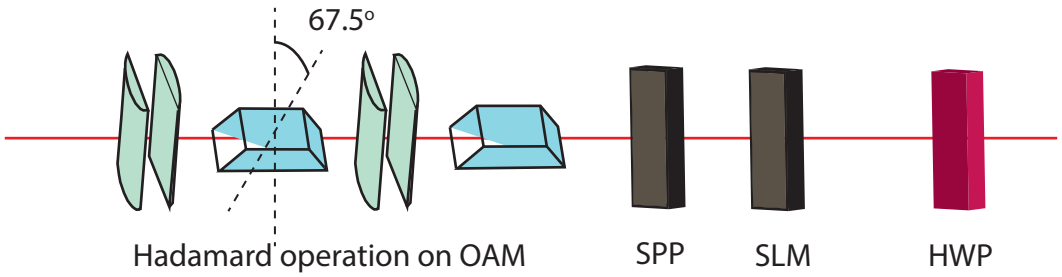

Figure 3.1: *Four-dimensional QFT on Polarization-OAM space*: The permuted wave is sent in as input, and first passes through a Hadamard for OAM modes, followed by a phase operation on OAM using a SPP and SLM, and Hadamard on polarization using a HWP.

Global phase can be neglected, and hence orienting a HWP at an angle 22.5° is sufficient to perform a Hadamard operation on polarization DOF. The next matrix,$(\mathbb{1}_2 \oplus D_2)$, is a polarization dependent phase operation on OAM modes, which can be realized by a combination of Spiral Phase Plate (SPP) which adds a specified value of l ($l = +1$ in this case) to all modes and a SLM, as SLMs are polarization sensitive. Now, $(\mathbb{1}_2 \otimes F_2)$ is a Hadamard operation on OAM modes, which can be realized using $\pi/2$-mode converters and Dove prism (see Fig. 3.1). This setup was already demonstrated by Song *et al.* [Song 15]. Note that this implementation uses one spatial mode and makes use of the internal DOFs of photon to perform a four-dimensional QFT. If the choice of basis is interchanged, the order in which the QFT operations are performed to the beam also reverses, along with a different permutation matrix.

3.1.1 Permutation on 4-dimensions

In Eq. 3.1, P_4 is the permutation matrix and is given by,

$$P_4 = \left[\begin{array}{c|c} 1 & \\ & 1 \\ \hline 1 & \\ & 1 \end{array}\right]. \tag{3.3}$$

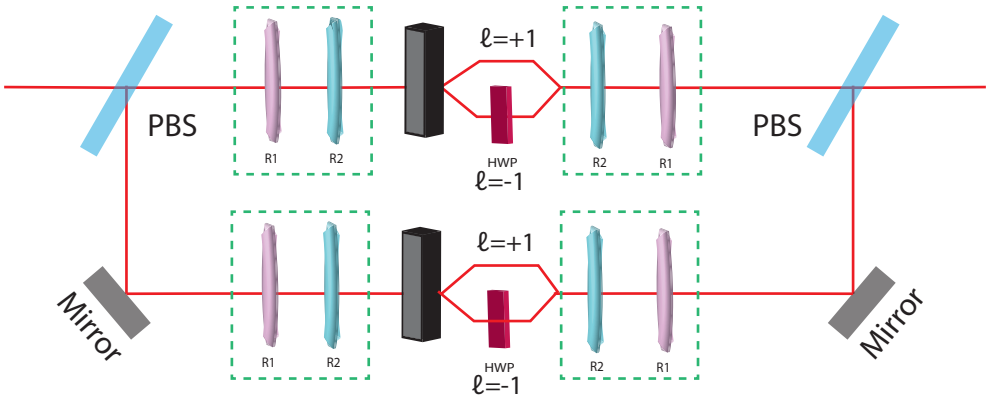

Figure 3.2: *Four-dimensional permutation on Polarization-OAM space*

This is a Polarization-OAM swap operation, due to the choice of our basis, and can be decomposed as

$$P_4 = \left[\begin{array}{cc|cc} 1 & & & \\ & 1 & & \\ \hline & & & 1 \\ & & 1 & \end{array}\right] \left[\begin{array}{cc|cc} 1 & & & \\ & & & 1 \\ \hline & & 1 & \\ & 1 & & \end{array}\right] \left[\begin{array}{cc|cc} 1 & & & \\ & 1 & & \\ \hline & & & 1 \\ & & 1 & \end{array}\right]$$
$$= (\mathbb{1}_2 \oplus \sigma_1) \left[\begin{array}{cc|cc} 1 & & & \\ & & & 1 \\ \hline & & 1 & \\ & 1 & & \end{array}\right] (\mathbb{1}_2 \oplus \sigma_1). \tag{3.4}$$

Here, σ_1 is the Pauli matrix which acts on the OAM subspace of photon to flip the OAM mode $l = 1$ to $l = -1$ and vice-versa. To realize this experimentally, a Polarizing Beam Splitter (PBS) is used to split the H and V components of polarization, and then a mirror is placed on the spatial mode corresponding to V to perform a reflection of OAM modes. The next matrix is a similar flipping operation, but acting on the polarization subspace of the photon. To realize this, Mirhosseini *et al.* scheme (see Section 2.9) can be used to sort OAM values, and then a HWP can be placed in the mode corresponding to $l = -1$. Hence, it requires 2 each of PBS, mirror, HWP, Fan-out SLM, and 7 custom made refractive elements required for log-polar mapping to completely realize the four-dimensional Polarization-OAM swap operation (see Fig. 3.2).

3.2 Eight-dimensional QFT

In order to implement the eight-dimensional QFT operation, we look at two different choices of n_s and n_i. Increasing the number of spatial modes to $n_s = 2$ from the

previous case of implementing F_4 is the first choice that we make. This sets $n_i = 4$, with two polarization DOFs and two OAM DOFs respecively. Applying adapted Torma's scheme yields,

$$F_8 = (F_2 \otimes \mathbb{1}_4)(\mathbb{1}_4 \oplus D_4)(\mathbb{1}_2 \otimes F_4)P_8. \tag{3.5}$$

where D_4 is a diagonal matrix with complex entries $(1, \omega, \omega^2, \omega^3)$. Here, $(F_2 \otimes \mathbb{1}_4)$ is a Hadamard operation on the spatial modes, which can be easily implemented using a 50:50 beam splitter and two phase shifters so that

$$F_2 = \frac{1}{\sqrt{2}} \begin{bmatrix} 1 & 0 \\ 0 & -i \end{bmatrix} \begin{bmatrix} 1 & i \\ i & 1 \end{bmatrix} \begin{bmatrix} 1 & 0 \\ 0 & -i \end{bmatrix}. \tag{3.6}$$

Now, $(\mathbb{1}_4 \oplus D_4)$ is a diagonal unitary operation on polarization and OAM modes on the second spatial mode. D_4 can be expressed as

$$D_4 = \begin{bmatrix} 1 & 0 \\ 0 & \omega^2 \end{bmatrix} \otimes \begin{bmatrix} 1 & 0 \\ 0 & \omega \end{bmatrix}, \tag{3.7}$$

where the first block is the operation of a waveplate on polarization and the second block is the operation of a SLM on the OAM modes (similar to the diagonal matrix realization in the four-dimensional QFT case). In the specific case of diagonal matrices powers of ω, an SLM can also be substituted with two Dove prisms and an appropriate phase shifter. Finally, $(\mathbb{1}_2 \otimes F_4)$ is the four-dimensional QFT operation on Polarization-OAM subspace that was realized in Section 3.1.

We will now choose $n_s = 4$ and $n_i = 2$ for realization of F_8. Specifically, we choose polarization as the internal DOF. In that case,

$$F_8 = (F_4 \otimes \mathbb{1}_2)(\mathbb{1}_2 \oplus D_2 \oplus D_2^2 \oplus D_2^3)(\mathbb{1}_4 \otimes F_2)P_8. \tag{3.8}$$

where D_2 is a diagonal matrix with complex entries $(1, \omega)$. Here, $(F_4 \otimes \mathbb{1}_2)$ is a QFT operation on four spatial modes, which can be realized using four beam splitters, phase shifters and appropriate spatial permutations [Törmä 96]. $(\mathbb{1}_2 \oplus D_2 \oplus D_2^2 \oplus D_2^3)$ corresponds to diagonal unitary operations on polarization DOF in second, third and fourth spatial modes respectively, which can be realized using appropriate waveplates 2.2.2. Finally, $(\mathbb{1}_4 \otimes F_2)$ can be realized using a HWP oriented at an angle 22.5°, at each of the spatial modes.

3.2.1 Permutation on 8-dimensions

In Eq. 3.5, P_8 is a permutation matrix that rearranges the columns of the decomposition obtained so as to get back F_8, and is given by,

$$P_8 = \left[\begin{array}{cccc|cccc} 1 & & & & & & & \\ & 1 & & & & & & \\ & & & & 1 & & & \\ & & & & & & & 1 \\ \hline & 1 & & & & & & \\ & & & 1 & & & & \\ & & & & & 1 & & \\ & & & & & & & 1 \end{array}\right]. \tag{3.9}$$

For a purely spatial based scheme, this matrix can be achieved by physically permuting the spatial modes as per the transformation, if implemented using fiber couplers, or by exploiting 3-D laser writing techniques to fabricate directional couplers of suitable spatial configuration on a borosilicon glass substrate [Crespi 16]. Here, we choose the basis for the matrices involved by including the internal degrees of freedom of the photon as well. Hence, permutation is achieved by a combination of physical permutation, waveplates and SLMs. The matrix P_8 can be expressed as,

$$\begin{aligned} P_8 &= \left(\left[\begin{array}{cc|cc} 1 & & & \\ & & 1 & \\ \hline & 1 & & \\ & & & 1 \end{array}\right] \otimes \mathbb{1}_2 \right) \times \left[\begin{array}{cccc|cccc} 1 & & & & & & & \\ & & 1 & & & & & \\ & 1 & & & & & & \\ & & & & & 1 & & \\ \hline & & & & 1 & & & \\ & & & & & & 1 & \\ & & & & & 1 & & \\ & & & & & & & 1 \end{array}\right] \\ &= (P_4 \otimes \mathbb{1}_2)(\mathbb{1}_2 \otimes P_4). \end{aligned} \tag{3.10}$$

First, let us consider the case where $n_s = 2$ and $n_i = 4$. Here, $(P_4 \otimes \mathbb{1}_2)$ acts on the spatial-polarization subspace and leaves the OAM modes unchanged. This matrix can be expressed as in Eq. 3.4, with the basis changed from polarization-OAM to spatial-polarization. Hence, it can be achieved experimentally using a PBS with a σ_1 operation on the polarization states only in the second spatial mode during input as well as output. σ_1 operation on polarization modes can be achieved by using a HWP.

The next matrix $(\mathbb{1}_2 \otimes P_4)$ corresponds to a P_4 operation on the polarization-OAM subspace as discussed previously in Section 3.1. Such a P_4 operation is performed in both the spatial modes.

Now, we consider the case where $n_s = 4$ and $n_i = 2$. In this case, $(P_4 \otimes \mathbb{1}_2)$ acts only on the spatial subspace and leaves the polarization DOF unchanged. A spatial permutation can be achieved by physically permuting the modes, as discussed earlier. It is evident that only second and third spatial modes are switched by the action of P_4. The next matrix in the sequence, $(\mathbb{1}_2 \otimes P_4)$, also includes the polarization DOF. The first block represents the subspace spanned by spatial modes 1 and 2, while the second block represents the subspace spanned by spatial modes 3 and 4. Hence, realizing this matrix reduces to placing two PBS with σ_1 operations (as discussed in $n_s = 2$, $n_i = 4$ case) between spatial modes $(1, 2)$ and $(3, 4)$ respectively.

3.3 Twelve-dimensional QFT

Physical realization of the 12×12 QFT matrix can be achieved using the proposed scheme for various combinations of n_s, n_p and n_o. Here, we choose $n_s = 2$, $n_p = 2$ and $n_o = 3$. Applying adapted Torma's scheme yields,

$$F_{12} = (F_2 \otimes \mathbb{1}_6)(\mathbb{1}_6 \oplus D_6)(\mathbb{1}_2 \otimes F_6)P_{12}. \tag{3.11}$$

where D_6 is a diagonal matrix with complex entries $(1, \omega, \omega^2, \omega^3, \omega^4, \omega^5)$. Here, $(F_2 \otimes \mathbb{1}_6)$ is an operation on the spatial subspace and is realized using a 50:50 beam splitter and two $\pi/2$ phase shifters. The next matrix, $(\mathbb{1}_6 \oplus D_6)$, is a phase shift in the second spatial mode, performed on the polarization-OAM subspace. D_6 can be re-expressed as

$$D_6 = \begin{bmatrix} 1 & 0 \\ 0 & \omega^3 \end{bmatrix} \otimes \begin{bmatrix} 1 & 0 & 0 \\ 0 & \omega & 0 \\ 0 & 0 & \omega^2 \end{bmatrix}. \tag{3.12}$$

The first block is a phase operation on the polarization DOF, which is realized using a suitable waveplate. The next block is a diagonal unitary operation on three OAM modes, which is realized using two Dove prisms rotated at appropriate angles. In $(\mathbb{1}_2 \otimes F_6)$, F_6 is a QFT operation on polarization-OAM subspace and can be further decomposed as follows,

$$F_6 = (F_2 \otimes \mathbb{1}_3)(\mathbb{1}_3 \oplus D_3)(\mathbb{1}_2 \otimes F_3)P_6. \tag{3.13}$$

Here, $(F_2 \otimes \mathbb{1}_3)$ is again a Hadamard operation on polarization modes, which can be achieved using a HWP rotated at an angle of 22.5° (see Section 3.1). $(\mathbb{1}_3 \oplus D_3)$ is a diagonal unitary operation on OAM, realized using two rotated Dove prisms and phase shifter. Finally, $(\mathbb{1}_2 \otimes F_3)$ is a three-dimensional QFT operation on OAM modes. Now, we discuss the realization of three-dimensional QFT using OAM modes.

3.3.1 QFT of three OAM modes

Realization of arbitrary unitary operation on OAM modes is usually done by splitting the different modes spatially using beam splitters and then performing relevant phase operations on the corresponding OAM modes, using a setup referred to as OAM sorter (see Section 2.4). However, this splitting further reduces the fidelity of the output state. Hence, it is always desirable that such operations can be performed in a single beam carrying a superposition of OAM modes. A two-dimensional QFT can be performed on the specific OAM modes with azimuthal indices -1 and 1 using astigmatic mode converter setups consisting of cylindrical lenses and Dove prisms [Song 15]. In the case of unitary operations for OAM modes greater than two, there are some inherent constraints. The main constraint for performing such operations for multiple OAM modes is related to the Position-OAM mapping of the beam under consideration [Pinnell 19]. For Laguerre-Gaussian modes with p=0, azimuthal indices corresponding to $-l$ and $+l$ are mapped to the same spatial position, and differ only in the handedness of rotation. This feature makes it hard to perform phase operations on individual $-l$ or $+l$ modes.

To realize QFT of three OAM modes, we derive a mathematical relation between a general $\mathbb{SU}(3)$ matrix (of which Quantum Fourier Transform is a special case), and $\mathbb{SO}(3)$ matrices. It requires eight parameters to characterize a general $\mathbb{SU}(3)$ matrix, and three parameters to characterize a general $\mathbb{SO}(3)$ matrix (Euler angle decomposition). More formally,
Theorem: Let O_1 and $O_2 \in \mathbb{SO}(3)$, and $M \in \mathbb{SU}(3)$. Then,

$$M = O_1 \, D \, O_2, \tag{3.14}$$

where D is a diagonal unitary matrix.
Proof:
Any arbitrary square unitary matrix U can be expressed as a combination of two real square matrices A and B as $U = A + iB$. Note that A and A^T have the same characteristic polynomial, resulting in same eigenvalues. This means that $[A, A^T] = 0$. This holds for B as well. Now, unitarity of U implies

$$\begin{aligned} UU^\dagger &= \mathbb{1} = (A + iB)(A^T - iB^T), \\ U^\dagger U &= \mathbb{1} = (A^T - iB^T)(A + iB), \end{aligned} \tag{3.15}$$

which yields the following two equations,

$$AA^T + BB^T - i(AB^T - BA^T) = \mathbb{1}, \tag{3.16}$$

$$A^TA + B^TB + i(A^TB - B^TA) = \mathbb{1}. \tag{3.17}$$

From Eq.(3.16) and Eq.(3.17), we see that the LHS of both the equations are a composition of symmetric and anti-symmetric parts. Since we have $\mathbb{1}$ in the RHS, the anti-symmetric part should be zero. So, we have

$$\begin{aligned} AA^T + BB^T &= \mathbb{1}, \\ A^TA + B^TB &= \mathbb{1}, \end{aligned} \tag{3.18}$$

which implies that $[AA^T, BB^T] = 0$ (or AA^T commutes with BB^T) and $[A^TA, B^TB] = 0$ (or A^TA commutes with B^TB). Hence, we see that both A and B are diagonalized by the same left singular and right singular vectors,

$$\begin{aligned} A &= O_1\Lambda^A O_2, \\ B &= O_1\Lambda^B O_2. \end{aligned} \tag{3.19}$$

Writing U in terms of A and B now,

$$U = O_1(\Lambda^A + i\Lambda^B)O_2. \tag{3.20}$$

Here, O_1 and O_2 here are real orthogonal matrices which can be characterized by 3 independent parameters, and the sum in between is a diagonal unitary matrix characterized by 2 independent parameters.

The optical elements that perform rotation of OAM modes are usually expressed in the Schwinger's basis which has the following generators,

$$J_1 = \begin{bmatrix} 0 & 1 & 0 \\ 1 & 0 & 1 \\ 0 & 1 & 0 \end{bmatrix}, \; J_2 = \begin{bmatrix} 0 & -i & 0 \\ i & 0 & -i \\ 0 & i & 0 \end{bmatrix}, \quad and \; J_3 = \begin{bmatrix} 2 & 0 & 0 \\ 0 & 0 & 0 \\ 0 & 0 & -2 \end{bmatrix}, \tag{3.21}$$

corresponding to OAM values $\{2, 0, -2\}$ [Sakurai 11]. LG modes are characterized using this OAM value (l) and a radial index p, which is defined as the minimum value of n_1 and n_2 oscillator states that make up the value of l (Eq.2.86). Here, the p indices are 0, 1, and 0 respectively. Any matrix in the Schwinger's basis can be parameterized using any two of these generators so that,

$$L(\alpha, \beta, \gamma) = e^{-i\alpha\hat{J}_3}e^{-i\beta\hat{J}_1}e^{-i\gamma\hat{J}_3}. \tag{3.22}$$

Introducing an additional phase of $e^{i\alpha J_3}$, we get

$$L(\alpha, \beta, \gamma) = e^{-i\alpha\hat{J}_3}e^{-i\beta\hat{J}_1}e^{i\alpha\hat{J}_3} \times e^{-i(\gamma+\alpha)\hat{J}_3}. \tag{3.23}$$

The first three operators in the RHS of Eq.3.23 represents the matrix $\mathbb{J}_1(\theta)$ in Eq. 2.101, and can be implemented using not more than 7 cylindrical lenses and 3 convex lenses [Ameen Yasir 17]. The last operator here can be implemented using 2 Dove prisms. Now, the generators of $\mathbb{SO}(3)$ in the computational basis are the following,

$$S_1 = \begin{bmatrix} 0 & 0 & 0 \\ 0 & 0 & i \\ 0 & -i & 0 \end{bmatrix}, \; S_2 = \begin{bmatrix} 0 & 0 & -i \\ 0 & 0 & 0 \\ i & 0 & 0 \end{bmatrix}, \quad and \; S_3 = \begin{bmatrix} 0 & i & 0 \\ -i & 0 & 0 \\ 0 & 0 & 0 \end{bmatrix}. \tag{3.24}$$

So, any arbitrary $\mathbb{SO}(3)$ operation can be performed on the OAM modes by establishing a unitary transformation between these two generator sets. The unitary operation that connects these matrices is the following,

$$U = \begin{bmatrix} 1 & 0 & i \\ 0 & 1 & 0 \\ -1 & 0 & i \end{bmatrix}, \tag{3.25}$$

and satisfies the following relation,

$$US_iU^\dagger = J_i \quad (i = 1, 2, 3) \tag{3.26}$$

Realizing the matrix U thus enables us to use already available optical transformations for the Schwinger basis. This matrix can be realized using an SLM, thus enabling interconversion of basis. Thus, three-dimensional QFT can be realized using cylindrical lenses, Dove prisms, convex lenses and SLMs.

3.3.2 Permutation on 12-dimensions

The last part remaining is the realization of the permutation matrices involved in the decomposition. In this particular case, we have $P_{fin} = (\mathbb{1}_2 \otimes P_6)P_{12}$. Here,

$$P_{12} = \left[\begin{array}{cccc|cccc} 1 & & & & & & & \\ & & 1 & & & & & \\ & & & 1 & & & & \\ & & & & 1 & & & \\ & & & & & 1 & & \\ & & & & & & & 1 \\ \hline & 1 & & & & & & \\ & & & 1 & & & & \\ & & & & 1 & & & \\ & & & & & & 1 & \\ & & & & & & & 1 \end{array}\right], \tag{3.27}$$

and

$$P_6 = \left[\begin{array}{ccc|ccc} 1 & & & & & \\ & & 1 & & & \\ & & & & & 1 \\ \hline & 1 & & & & \\ & & & & 1 & \\ & & & & & 1 \end{array}\right]. \tag{3.28}$$

We find that $P_{12} = P_{row}(\mathbb{1}_2 \otimes P_6)$, with

$$P_{row} = \left(\left[\begin{array}{ccc|ccc} 1 & & & & & \\ & 1 & & & & \\ & & & & & 1 \\ \hline & & & & 1 & \\ & & & 1 & & \end{array}\right]\left[\begin{array}{ccc|ccc} 1 & & & & & \\ & & & & 1 & \\ & & & 1 & & \\ \hline & & & & & \\ & 1 & & & & \end{array}\right]\left[\begin{array}{ccc|ccc} 1 & & & & & \\ & 1 & & & & \\ & & & & & 1 \\ \hline & & & & & \\ & & & 1 & & \end{array}\right]\right) \otimes \mathbb{1}_3. \tag{3.29}$$

P_{row} can be implemented as discussed previously in the section for realization of eight-dimensional QFT. Now, P_6 can be decomposed to $(\mathbb{1}_2 \oplus \sigma_1 \oplus \mathbb{1}_2)(P_3(132) \oplus P_3(213))$, where

$$P_3(132) = \begin{bmatrix} 1 & & \\ & & 1 \\ & 1 & \end{bmatrix} \text{ and } P(213) = \begin{bmatrix} & 1 & \\ 1 & & \\ & & 1 \end{bmatrix}, \tag{3.30}$$

which can be realized using a combination of waveplates and SLMs.

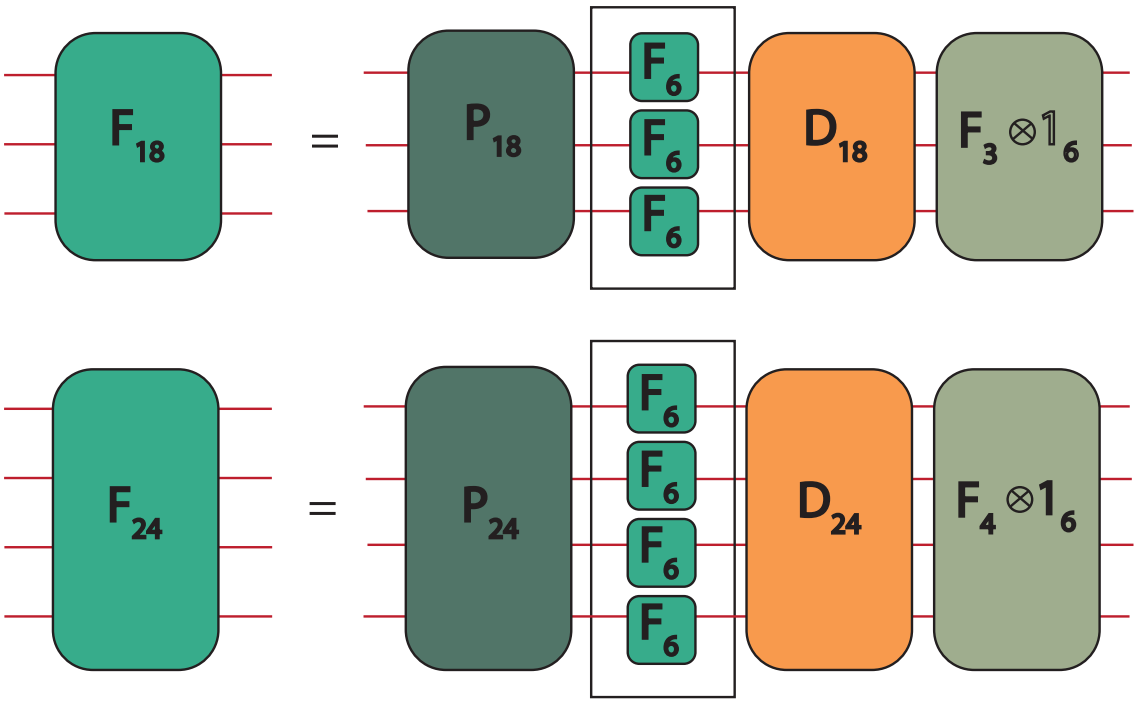

Figure 3.3: *Modularity presented by the scheme*: Implementing F_{18} and F_{24} becomes easier as combining required number of F_6 operations with appropriate permutations and spatial QFT is equivalent to these higher dimensional QFT operations.

3.4 Cost analysis

For implementation of the four-dimensional QFT, we require 25 components which consists of 4 cylindrical lenses, 2 Dove prisms, 1 SPP, 3 SLMs, 3 HWPs, 2 PBS, 8 refractive elements and 2 mirrors. By increasing the number of spatial modes to two, the four-dimensional QFT can be combined in a modular array to perform the eight-dimensional QFT, thus requiring 50 elements for transformation of the internal DOFs. This estimate is after including the permutation on polarization-OAM subspace. Apart from the internal transformations, we require one SPP and two Dove prisms for diagonal unitary operation and 6 beam splitters (5 PBS, for permutation, and a 50:50 beam splitter for Hadamard transformation) for spatial transformations. In contrast, the method presented in [Crespi 16] (using Torma's scheme) requires a total of 12 beam splitters to do the same transformation, with use of no internal elements.

Now, choosing $n_s = 4$ and $n_i = 2$ (polarization DOF) for realizing eight-dimensional QFT requires 2 PBS and 4 HWPs for permutation, 4 HWPs for QFT on polarization at each spatial modes, 3 suitable waveplates for diagonal unitary transformation and 4 beam splitter devices for four-dimensional QFT of spatial modes. This implementation also requires six beam splitters, which means lesser number of beam splitters as compared to Torma's scheme.

To implement a three-dimensional QFT, we require 14 cylindrical lenses, 6 Dove prisms, a phase shifter, 4 SLMs and 6 lenses. This means that in order to implement the twelve-dimensional QFT, we require 28 cylindrical lenses, 20 SLMs, 18 Dove prisms, 12 lenses, 9 waveplates, 8 SPPs, and 4 phase shifters to implement the internal transformations (which is a total of 99 internal elements), along with 2 beam splitters and 2 phase shifters for spatial transformation. This is in contrast to the 132 beam splitters required to implement a twelve-dimensional transformation using available schemes [Reck 94, Clements 16]. Our adaptation of Torma's scheme is advantageous for the fact that it requires lesser number of beam splitting operations and hence provides an easier way to implement transformations without having to align $\mathcal{O}(N^2)$ beam splitters.

Chapter 4

Conclusion

Quantum Fourier Transform is an important unitary operation for various Quantum information processing schemes and machine learning methods. The ability to realize such an operation for higher dimensional Hilbert spaces could help in demonstrating quantum supremacy over its classical counterparts, whether it is computing or cryptography. We hope that this work could be extended to improve the scalability of the scheme for realizing higher dimensional QFT operations.

The design that we present for implementing QFT is particularly advantageous due to its modular structure, which means that lower dimensional QFT operations can be combined to realize a higher dimensional QFT operation. In order to realize 12 dimensional QFT of input states, two 6 dimensional QFT operations acting solely on internal modes can be combined in two independent spatial modes to generate the transformation. In fact, any multiple of n_i can be implemented, given that operation on n_i internal modes are possible in a single beam. Realizing N dimensional QFT operations on the OAM carried by a single beam still remains a challenge, and could be addressed by constructions involving SLMs.

Machine learning methods like Generative Adversarial Learning, which is a neural architecture consisting of three independent neural networks correcting and evolving from each others errors, can be combined with the concept of inverse optical design to generate novel metamaterials that could transform an arbitrary dimensional OAM space to any desirable OAM spectrum [Liu 18, Zhang 19]. This could mean that more dimensions can be controlled inside a single beam itself with lesser number of optical elements, providing more fidelity to the output states and less complexity for experimental realization. Optimizing the choice of basis according to lesser complexity of experimental implementation setup and lesser number of components is a challenge, and could possibly be solved using machine learning methods.

We have adapted an algorithm for realizing experimental setups for arbitrary dimensional Quantum Fourier Transform (QFT) by incorporating internal modes of light. This means that the operations on internal degrees of freedom like polarization,

OAM, and time bins can in effect reduce the number of spatial modes involved for higher dimensional realizations of QFT, thus helping in reducing the number of beam splitters to be included in the experimental setup. The algorithm was demonstrated for a 12 dimensional QFT transformation which required only 2 beam splitters in place of 132, which reduces the overhead loss of splitting the beam multiple times, and that of the beam encountering different number of optical elements in different arms of the experimental setup. However, the total number of components are higher than other available schemes due to addition of internal transformations. Finally, realization of permutation matrices involving internal modes is difficult, and a general decomposition algorithm for separating the action of permutation onto spatial permutation and internal permutation is yet to be achieved. This would help in assessing the exact cost of realizing any higher dimensional QFT operation with respect to the number of components required.

Bibliography

[Allen 92] Les Allen, Marco W Beijersbergen, RJC Spreeuw & JP Woerdman. *Orbital angular momentum of light and the transformation of Laguerre-Gaussian laser modes.* Physical review A, vol. 45, no. 11, page 8185, 1992.

[Allen 99] L Allen, J Courtial & MJ Padgett. *Matrix formulation for the propagation of light beams with orbital and spin angular momenta.* Physical Review E, vol. 60, no. 6, page 7497, 1999.

[Ameen Yasir 17] P. A. Ameen Yasir & J. Solomon Ivan. *Realization of first-order optical systems using thin lenses of positive focal length.* Journal of the Optical Society of America A, vol. 34, no. 11, page 2007, 2017.

[Arrizón 07] Victor Arrizón, Ulises Ruiz, Rosibel Carrada & Luis A. González. *Pixelated phase computer holograms for the accurate encoding of scalar complex fields.* Journal of the Optical Society of America A, vol. 24, no. 11, page 3500, 2007.

[Beijersbergen 93] Marco W Beijersbergen, Les Allen, HELO Van der Veen & JP Woerdman. *Astigmatic laser mode converters and transfer of orbital angular momentum.* Optics Communications, vol. 96, no. 1-3, pages 123–132, 1993.

[Berkhout 10] Gregorius CG Berkhout, Martin PJ Lavery, Johannes Courtial, Marco W Beijersbergen & Miles J Padgett. *Efficient sorting of orbital angular momentum states of light.* Physical review letters, vol. 105, no. 15, page 153601, 2010.

[Clements 16] William R. Clements, Peter C. Humphreys, Benjamin J. Metcalf, W. Steven Kolthammer & Ian A. Walsmley. *Optimal design for universal multiport interferometers.* Optica, vol. 3, no. 12, page 1460, 2016.

[Cooley 65] James W. Cooley & John W. Tukey. *An Algorithm for the Machine Calculation of Complex Fourier Series.* Mathematics of Computation, vol. 19, no. 90, page 297, 1965.

[Crespi 16] Andrea Crespi, Roberto Osellame, Roberta Ramponi, Marco Bentivegna, Fulvio Flamini, Nicolò Spagnolo, Niko Viggianiello, Luca Innocenti, Paolo Mataloni & Fabio Sciarrino. *Suppression law of quantum states in a 3D photonic fast Fourier transform chip.* Nature communications, vol. 7, no. 1, pages 1–8, 2016.

[Deutsch 92] David Deutsch & Richard Jozsa. *Rapid solution of problems by quantum computation.* Proceedings of the Royal Society of London. Series A: Mathematical and Physical Sciences, vol. 439, no. 1907, pages 553–558, 1992.

[Dhand 15] Ish Dhand & Sandeep K. Goyal. *Realization of arbitrary discrete unitary transformations using spatial and internal modes of light.* Physical Review A - Atomic, Molecular, and Optical Physics, vol. 92, no. 4, pages 1–9, 2015.

[Gadway 08] Bryce R Gadway, John W Noe & Martin G Cohen. *Universal quantum gates for order N= 1 OAM states.* In Frontiers in Optics, page JSuA1. Optical Society of America, 2008.

[Leach 02] Jonathan Leach, Miles J Padgett, Stephen M Barnett, Sonja Franke-Arnold & Johannes Courtial. *Measuring the orbital angular momentum of a single photon.* Physical review letters, vol. 88, no. 25, page 257901, 2002.

[Liu 18] Zhaocheng Liu, Dayu Zhu, Sean P. Rodrigues, Kyu Tae Lee & Wenshan Cai. *Generative Model for the Inverse Design of Metasurfaces.* Nano Letters, vol. 18, no. 10, pages 6570–6576, 2018.

[Lloyd 13] Seth Lloyd, Masoud Mohseni & Patrick Rebentrost. *Quantum algorithms for supervised and unsupervised machine learning.* arXiv preprint arXiv:1307.0411, 2013.

[Mariantoni 11] Matteo Mariantoni, H. Wang, T. Yamamoto, M. Neeley, Radoslaw C. Bialczak, Y. Chen, M. Lenander, Erik Lucero, A. D. O'Connell, D. Sank, M. Weides, J. Wenner, Y. Yin, J. Zhao, A. N. Korotkov, A. N. Cleland & John M. Martinis. *Implementing the quantum von Neumann architecture with superconducting circuits.* Science, vol. 334, no. 6052, pages 61–65, 2011.

[Mirhosseini 13] Mohammad Mirhosseini, Mehul Malik, Zhimin Shi & Robert W. Boyd. *Efficient separation of the orbital angular momentum eigenstates of light.* Nature Communications, vol. 4, pages 1–6, 2013.

[Moreno 04] Ivan Moreno. *Jones matrix for image-rotation prisms.* Applied optics, vol. 43, no. 17, pages 3373–3381, 2004.

[Pinnell 19] Jonathan Pinnell, Valeria Rodríguez-Fajardo & Andrew Forbes. *Single-step shaping of the orbital angular momentum spectrum of light.* Optics Express, vol. 27, no. 20, page 28009, 2019.

[Reck 94] Michael Reck, Anton Zeilinger, Herbert J Bernstein & Philip Bertani. *Experimental realization of any discrete unitary operator.* Physical review letters, vol. 73, no. 1, page 58, 1994.

[Roetteler 98] Martin Roetteler & Thomas Beth. *Polynomial-time solution to the hidden subgroup problem for a class of non-abelian groups.* arXiv preprint quant-ph/9812070, 1998.

[Ruiz-Perez 17] Lidia Ruiz-Perez & Juan Carlos Garcia-Escartin. *Quantum arithmetic with the quantum Fourier transform.* Quantum Information Processing, vol. 16, no. 6, 2017.

[Sakurai 11] Jun John Sakurai & Jim Napolitano. *Modern quantum physics*, 2011.

[Scully 02] Marlan O. Scully & M. Suhail Zubairy. *Cavity QED implementation of the discrete quantum Fourier transform.* Physical Review A - Atomic, Molecular, and Optical Physics, vol. 65, no. 5, page 4, 2002.

[Shor 97] Peter W Shor. *Polynomial-Time Algorithms for Prime Factorization and Discrete Logarithms on a Quantum Computer.* SIAM Journal on Computing, vol. 26, no. 5, pages 1484–1509, 1997.

[Simon 89] R. Simon & N. Mukunda. *Universal SU(2) gadget for polarization optics.* Physics Letters A, vol. 138, no. 9, pages 474–480, 1989.

[Simon 90] R Simon & N Mukunda. *Minimal three-component SU (2) gadget for polarization optics.* Physics Letters A, vol. 143, no. 4-5, pages 165–169, 1990.

[Simon 93] R. Simon, N. Mukunda & K. Sundar. *Twisted Gaussian Schell-model beams I Symmetry structure and normal-mode spectrum.*

Journal of the Optical Society of America A, vol. 10, no. 9, page 2008, 1993.

[Song 15] Xinbing Song, Yifan Sun, Pengyun Li, Hongwei Qin & Xiangdong Zhang. *Bell's measure and implementing quantum Fourier transform with orbital angular momentum of classical light.* Scientific reports, vol. 5, no. 1, pages 1–8, 2015.

[Sudarshan 85] E. C.G. Sudarshan, N. Mukunda & R. Simon. *Realization of first order optical systems using thin lenses.* Optica acta, vol. 32, no. 8, pages 855–872, 1985.

[Törmä 96] P Törmä, I Jex & S Stenholm. *Beam splitter realizations of totally symmetric mode couplers.* Journal of Modern Optics, vol. 43, no. 2, pages 245–251, 1996.

[Weinstein 01] Y. S. Weinstein, M. A. Pravia, E. M. Fortunato, S. Lloyd & D. G. Cory. *Implementation of the quantum Fourier transform.* Physical Review Letters, vol. 86, no. 9, pages 1889–1891, 2001.

[Yasir 14] PA Ameen Yasir & J Solomon Ivan. *Realization of first-order optical systems using thin convex lenses of fixed focal length.* JOSA A, vol. 31, no. 9, pages 2011–2020, 2014.

[Zhang 19] Yuchao Zhang, Xiaodong Yang & Jie Gao. *Orbital angular momentum transformation of optical vortex with aluminum metasurfaces.* Scientific Reports, vol. 9, no. 1, pages 1–9, 2019.

[Zhou 13] Xiao Qi Zhou, Pruet Kalasuwan, Timothy C. Ralph & Jeremy L. O'brien. *Calculating unknown eigenvalues with a quantum algorithm.* Nature Photonics, vol. 7, no. 3, pages 223–228, 2013.